W-AM-Sym I-1

PARTIALLY-FOLDED INTERMEDIATES IN ACID-DENATURATION OF PROTEINS Anthony L. Fink, Linda J. Calciano, Yuji Goto, Takuzo Kurotsu, Daniel J. Palleros and Sally A. Swedberg, Department of Chemistry and Biochemistry, University of California, Santa Cruz, CA 95064.

Three major types of conformational behavior occur on acid denaturation, depending on the protein, the acid, the presence of salts or denaturant, and the temperature. The observed behavior ranges from no significant unfolding down to pH as low as 0.5, to unfolding in the vicinity of pH 3 or 4 followed by refolding to a compact, molten globule-like state at pH below 2, to direct transformation of the native state to the molten globule state. The particular behavior observed reflects the balance of attractive and repulsive forces, and can be converted from one type to another by the addition of anions or denaturants. Two types of intermediate states, both characterized by the presence of secondary structure and the absence of significant tertiary structure, but differing in their degree of compactness, are observed. Intermediates with similar properties are seen in kinetics experiments monitoring the refolding process which show the very rapid return of secondary structure. Characterization of the compact unfolded states by FTIR reveals the presence of some non-native secondary structure.

W-AM-Sym I-2

RESIDUAL STRUCTURE IN THE DENATURED STATE OF STAPHYLOCOCCAL NUCLEASE. David Shortle, Dept. of Biological Chemistry, The Johns Hopkins University School of Medicine, Baltimore, MD 21205.

W-AM-Sym I-3

IMMUNOCHEMICAL STUDIES OF FOLDING INTERMEDIATES
MICHEL E. GOLDBERG - Institut Pasteur - Paris - France

The refolding of the β_2 subunit of *E. coli* tryptophan synthase, unfolded with urea, guanidine or acid, has been investigated by means of a variety of optical probes (far and near UV circular dichroism, ANS binding, intrinsic fluorescence, fluorescence transfer and polarization of added fluorescence probes) and by the regain of the function. The kinetics of regain of the "native-like" signal for each probe shows that refolding of β chains proceeds through a timely sequence of steps with half reaction times ranging from less than 10 msec to over 15 min [1]. Using a panel of monoclonal antibodies (mAb) elicited against native β_2, and shown to bind efficiently to native β_2, we investigated the kinetics of appearance of the corresponding "native-like" epitopes during the folding process. The main results were that:

- 2 mAbs (Ig9 and Ig19) that recognize distinct epitopes on the N-terminal (F1) domain of native β_2, bind to early folding intermediates with rate and equilibrium association constants similar to those found for the association of the mAbs with native b_2[2,3].
- the epitope to Ig19 already appears within the molten globule, before the begining of the tight-packing of side chains (as seen by ANS release). The epitope to Ig9 appears together with the faster phase of tight packing[1].
- 3 other epitopes (2 on the C-terminal F2 domain, one on the hinge between F1 and F2) appear so rapidly ($t_{1/2}$ < 500 msec) during the folding of isolated F2 that their formation could not be obeserved[3].
- the epitope to Ig164 is contained in an 11 residue sequence of the hinge region between F1 and F2. The undecapeptide with this sequence was synthetised chemicaly; it binds to Ig164 with nearly the same affinity as native β_2[4]. 2D NMR studies on this peptide in solution indicate that it adopts, in normal aqueous buffer, a conformation with a β-turn also present in native β_2.

These results will be discussed in terms of movements within the molten globule that lead to the proper relative docking of secondary structure elements or of domains.

(1) Goldberg et al. (1990) FEBS Letters 263, 51-56
(2) Murry-Brelier & Goldberg (1988) Biochemistry, 27, 7633-7640
(3) Blond-Elguindi & Goldberg (1990) Biochemistry, 29, 2409-2417
(4) Larvor, Djavadi-Ohaniance, Friguet, Baleux & Goldberg, Mol. Immunol. in press

W-AM-Sym I-4

EQUILIBRIUM AND KINETICS OF FOLDING OF STAPHYLOCOCCAL NUCLEASE STUDIED BY PEPTIDE CIRCULAR DICHROISM SPECTRA

KUNIHIRO KUWAJIMA
Department of Polymer Science, Faculty of Science, Hokkaido University, Sapporo 060, Japan

The reversible equilibrium unfolding of staphylococcal nuclease A when treated with urea and the kinetics of unfolding and refolding induced by concentration jump of urea have been studied by the peptide circular dichroism spectra at pH 7.0 and 4.5°C. As Ca^{2+} and deoxythymidine 3',5'-diphosphate (pdTp) are both known to be specific ligands bound by the native protein, the reactions were investigated under four conditions, in which the solution contained (1) no ligand, (2) 10 mM $CaCl_2$, (3) 1 mM pdTp and (4) 1 mM pdTp plus 10 mM $CaCl_2$. The results obtained are summarized as follows. (1) The increases in stabilization free energy by the ligands are interpreted in terms of simple displacements of the unfolding equilibrium due to ligand binding to the native molecule. (2) At the first stage of kinetic refolding from the fully unfolded state, the peptide ellipticity changes rapidly within the dead time of stopped-flow measurement (15 ms), indicating accumulation of a transient intermediate. The intermediate of this protein is, however, remarkably less stable than those of other globular proteins previously studied in this respect. (3) Dependence of the folding and unfolding rates on urea concentration indicates considerable structural organization in the critical transition state of folding. However, the molecule in the transition state does not have capacity to bind Ca^{2+} and pdTp, as indicated by selective effect of the ligands on the unfolding rate constant. (4) There are at least four different phases in refolding kinetics in native conditions below 1 M urea. In the absence of pdTp, there are two phases in unfolding, while the presence of pdTp makes the unfolding obey the single-phase kinetics.

Characteristics of the transient intermediate and the transition state of protein folding are discussed from these results together with the results previously obtained for other globular proteins.

W-AM-A1

EFFECTS OF ω-CONOTOXIN (ω-CgTx) ON CALCIUM CURRENTS IN PEPTIDERGIC NERVE TERMINALS OF THE RAT NEUROHYPOPHYSIS. Xiaoming Wang, Steven N. Treistman and José R. Lemos. Worcester Foundation for Experimental Biology, Shrewsbury, MA 01545, USA

It is known that in nerve terminals there are at least two subtypes of voltage-sensitive calcium channels, the inactivating "NT-type" and the longer-lasting "L-type" (Lemos and Nowycky, 1989). Using "whole-cell" patch clamp techniques, we examined the effects of ω-CgTx on both of these calcium currents in the isolated peptidergic nerve terminals (6-8 μM in diameter) of the rat neurohypophysis. The two components of calcium currents can be differentiated by depolarizing pulses from two different holding potentials, -90 mV and -50 mV, respectively. ω-CgTx at doses of 0.01, 0.03, 0.1, 0.3 and 2 μM is perfused via a micropipette onto the individual terminal. At concentrations as low as 0.03 μM ω-CgTx can significantly reduce the "NT-type" calcium currents [peak currents reduced from -144.03 ± 18.07 pA (mean ± SEM) (n=8) to -91.98 ± 10.89 pA (n=8), $p<0.05$]. However, "L-type" calcium currents are not affected by ω-CgTx until at a dose of 0.3 μM [peak currents reduced from -46.89 ± 3.40 pA (n=10) to -28.24 ± 3.93 pA (n=6), $p<0.01$]. The reduction in either current amplitude by ω-CgTx does not result from a shift in their current-voltage relationships. Our results suggest that ω-CgTx can block both "NT-type" and "L-type" calcium channels in the neurohypophysial peptidergic nerve terminals, but the "NT-type" is more sensitive to ω-CgTx than the "L-type".

(Supported by PHS grant AA08003)

W-AM-A2

ω-CONOTOXIN INHIBITS A CA^{2+} CURRENT IN BOVINE CHROMAFFIN CELLS THAT DOES NOT SEEM TO BE N-TYPE. Cristina R. Artalejo, Robert, L. Perlman, & Aaron P. Fox. The University of Chicago, Dept. of Pharm/ Phys.

Two criteria are generally used to define N-type Ca channels. First, N-channels are sensitive to changes in holding potential. Changing the holding potential from -100 mV to -50 mV typically inactivates 60% or more of N-type current. The other criterion is the N-channel sensitivity to ω-CgTx. It has been suggested that ω-CgTx blocks N-type Ca channels exclusively. Bovine chromaffin cells have two types of Ca currents. The "standard" component is activated by brief depolarizations. The "facilitation" component is activated by prolonged pre-depolarizations to very positive potentials, or by repetitive small depolarizations in the physiological range. The "standard" component component is blocked by ω-CgTx in an irreversible manner, but shows no dependence on holding potential in the range from -40 mV to -100 mV. Thus, it is a channel unlike N-type in terms of holding potential dependence but that is sensitive to ω-CgTx. These studies suggest that current classification of Ca channels into T,N,L, & P types may be inadequate.

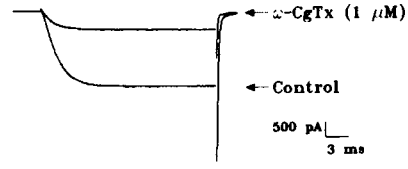

W-AM-A3

ACTIVATION OF ADENOSINE A_2 RECEPTORS POTENTIATES Ca CURRENT IN ACUTELY ISOLATED HIPPOCAMPAL CA3 PYRAMIDAL NEURONS. David J. Mogul and Aaron P. Fox (Intro. by M. Villereal)
Department of Pharmacological and Physiological Sciences
University of Chicago, Chicago, IL 60637 U. S. A.

Adenosine, released from tissues in response to various stimuli, has been found to exert diverse physiological effects. Previous studies of the effects of adenosine or its analogues have reported that adenosine decreases neuronal calcium current (i_{Ca}), presumably by acting on a high-threshold (N-type) component of i_{Ca} (Madison et al., 1987; Gross et al., 1989). We studied adenosine modulation of i_{Ca} using the whole-cell voltage clamp technique on acutely isolated guinea pig hippocampal pyramidal neurons from the CA3 region. We found that selective activation of individual adenosine receptors caused different i_{Ca} responses. When the A_2 receptor was activated through use of the A_2 agonist DPMA (50 nM), peak i_{Ca} increased at all potentials tested. Alternatively, when the A_2 receptor was activated by blocking the A_1 receptor with CPT (500 μM) and subsequent exposure to adenosine (50 μM), i_{Ca} from a holding potential = -100 mV was significantly potentiated at test potentials between -60 mV and -40 mV (below left). However, i_{Ca} was decreased at test potentials greater than -40 mV (below right). This potentiated current decayed only very slowly when A_2 receptor activation was withdrawn. This current was insensitive to the N-type Ca channel blocker ω-conotoxin (ω-CgTx) but was sensitive to Ni^{2+}. Ni^{2+} virtually abolished the entire fraction of current increase due to A_2 activation. Upon washout, the current rapidly returned to its elevated level. Only a decrease in i_{Ca} was observed upon exposure to the selective A_1 agonist, CPA. Study is continuing to determine the component(s) of i_{Ca} potentiated by A_2 activation or decreased by A_1 activation.

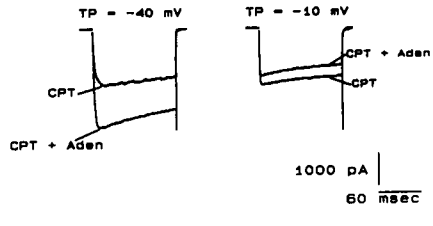

W-AM-A4

INACTIVATION OF CALCIUM CHANNELS IN RABBIT PORTAL VEIN (PV) MYOCYTES. R. H. Cox, A. J. Davidoff, D. Katzka and M. Morad. Dept. of Physiol. Univ. of PA, and Bockus Res. Inst. and CECS, Grad. Hosp., Phila., PA.

The characteristics of inactivation and recovery from inactivation were studied in enzymatically dispersed, whole cell clamped PV myocytes. I_{Ca} was recorded using as an internal solution (in mM) 120 CsCl, 20 TEACl, 5 MgATP, 14 EGTA, 10 HEPES and 0.01 cAMP. The time course of inactivation could be represented by two voltage-dependent time constants ($[Ca^{2+}]_o$=5mM, V=0mV: τ_{fast}=22±1 and τ_{slow}=88±6 msec). Increasing I_{Ca} by increasing $[Ca^{2+}]_o$ or with more negative potentials, decreased both τ_{fast} and τ_{slow}. With Ba^{2+} or Na^+ as charge carrier, inactivation was also represented by two voltage-dependent τs which were larger (5mM Ba^{2+} @ 0mV: τ_{fast} =48±6 and τ_{slow}=186±27 msec; 135mM Na^+ @ 0mV: τ_{fast}=63±9 and τ_{slow}=304±13 msec). With Ca^{2+} or Ba^{2+} both τs had minima (τ_{min}) near the voltage associated with maximum current (I_{max}), ie. ≈0mV. When Na^+ (135mM) was the charge carrier, voltages for I_{max} (-30 mV) and τ_{min} (0mV) did not correspond. Steady state inactivation (SSI) of I_{Ca} was performed by 2s conditioning pulses from -120 to +30mV, then stepping to the test voltage producing I_{max}. SSI of the Ca^{2+} channel had a half maximum value of -32±4mV for Ca^{2+}, -41±5mV for Ba^{2+} and -68±6 mV for Na^+. SSI had a slope factor of 6.5±0.2 mV per e-fold voltage change for Ca^{2+} or Ba^{2+} representing 4 equivalent charges and 13.5±0.7 mV for Na^+ representing 2 equivalent charges. The time course of recovery of I_{Ca} from inactivation was fit by two τs and the rate of recovery varied inversely with recovery voltage but was independent of the charge carrier. These results suggest that inactivation of the Ca^{2+} channel in PV myocytes exhibits both voltage and Ca^{2+} dependence. Unlike cardiac and neuronal Ca^{2+} channels, inactivation of the PV Ca^{2+} channel requires 2 equivalent charges for monovalents and 4 for divalents, suggesting that cation charge confers the voltage-dependency of channel inactivation.

(Supported by HL 16152 and HL 39388).

W-AM-A5

FOLLICLE STIMULATING HORMONE (FSH)-INDUCED ELEVATIONS OF CYTOSOLIC CALCIUM IN RAT SERTOLI CELLS

Eleonora Gorczynska, David J. Handelsman
Departments of Obstetrics and Gynecology and of Medicine, University of Sydney, Sydney NSW 2006, Australia

Sertoli cells create the blood-testis barrier and form the distinctive fluid microenvironment of the seminiferous tubules under major hormonal regulation by FSH. While previous studies have implicated cyclic AMP as a second messenger for FSH, the intracellular calcium level and its regulation have not been reported in these cells.

Freshly isolated Sertoli cells from 18-22 day old Wistar rats were loaded with 20 μM Fura 2-AM for 1 hr at 37 C and cytosolic calcium studied continuously by microfluorometry in a Hitachi 4010 fluorimeter. Analysis was performed on cytosolic calcium levels at 180 sec after application of agents or diluent control. Intracellular calcium concentration in unstimulated Sertoli cells was 103 ± 7 (SEM) nM (n=8 expts). Stimulation with ovine FSH (1000 ng S-16/ml) produced a gradual increase in cytosolic calcium levels rising to 192 ± 31 nM (n=7 expts; p=0.027 vs unstimulated). Pre-incubation for 20 min with nicardipine (50 μM), a blocker of voltage-gated calcium channels, produced a marked fall in the resting cytosolic calcium (20 ± 9 nM; n=4 expts) and totally abolished the FSH-induced rise in intracellular calcium (21 ± 8 nM). Another voltage-gated calcium channel blocker, verapamil (100 μM) had similar effects (69 ± 3 nM basal, 60 ± 8 post-FSH; n=4 expts each).

These findings indicate that activation of plasma membrane calcium channels occurs as a result of signal transduction from the FSH receptors on Sertoli cells. The relatively delayed response suggests that increased intracellular calcium may not be the principal second messenger for intracellular actions of FSH. Further studies are required to determine the intracellular mechanism of the FSH-induced rise in cytosolic calcium.

W-AM-A6

GUANINE NUCLEOTIDES MODULATE CALCIUM CURRENTS IN MARINE PARAMECIUM. J. Bernal and B.E. Ehrlich. Depts. of Medicine and Physiology, Univ. of CT, Farmington CT and Depto. de Fisiologia, Universidad de Aguascalientes, Mexico.

We have shown previously that guanine nucleotides modulate backward swimming behavior and the calcium action potential in the marine ciliate Paramecium calkinsi (Biophys. J. 53:21a, 1988; 55:39a, 1989). In order to show that these effects of the guanine nucleotides were indeed on calcium channels, calcium currents (ICa^{2+}) in the marine Paramecium were studied. Two microelectrode voltage clamp experiments were done. Cells were held at -80 mV and depolarizing pulses were applied to elicit the calcium currents. It was found that ICa^{2+} was activated at -20 mV and ICa^{2+}Max was seen at +20 mV. ICa^{2+} had an extracellular calcium dependence where the magnitude of ICa^{2+} increased as the extracellular calcium concentration was increased from 0.5 to 90 mM. ICa^{2+}Max shifted +10 mV along the voltage axis when the extracellular calcium concentration was increased 10 fold. Inorganic compounds ($NiCl_2$ at 50 uM and $CdCl_2$ at 1 mM) and organic compounds (naphthalene sulfonamides, W-7 and W12-Br at 100 uM and 2 uM, respectively) blocked ICa^{2+}. Hydrolyzable and non hydrolyzable analogs of guanine nucleotides were injected into voltage clamped cells when calcium and potassium currents were monitored. GTP increased the magnitude of the calcium current 35 % in a reversible manner whereas the injection of GTPγS irreversibly increased the calcium current 40 %. GDPβS had effects opposite to those of GTPγS. No shifts in ICa^{2+}Max were seen after injection of these compounds. Other experiments were done to see if the K^+ currents could be modified by the injected compounds. The total outward current did not change when GTPγS was injected into the cell. These results support the hypothesis that guanine nucleotides modulate the voltage-dependent calcium channel in Paramecium.

JB is a Fellow of AHA, CT affiliate. BEE is a PEW Scholar in the Biomedical Sciences.

W-AM-A7

PHARMACOLOGICAL AND INACTIVATION PROPERTIES DISTINGUISH TWO CALCIUM CURRENTS IN MOUSE PANCREATIC β-CELLS. W.F. Hopkins, L.S. Satin, and D.L. Cook, Depts. of Physiology/Biophysics and Medicine, Univ. of Washington and VA Medical Center, Seattle, WA 98108.

Neonatal rat pancreatic β-cells and insulin-secreting HIT cells each possess two voltage-dependent calcium currents (Satin and Cook, *Pflügers Arch.* **411**: 401-409, 1988; *Pflügers Arch.* **414**: 1-10, 1989). In contrast, adult mouse β-cells have been reported to possess only one type of calcium current. To explore this discrepancy, we studied calcium currents in adult mouse β-cells using the whole-cell variation of the patch clamp technique. When calcium currents were elicited with ten second test pulses to 0 millivolts from a holding potential of -100 millivolts, the time course of inactivation was well fit by the sum of two exponentials, although for some cells three exponentials yielded a better fit. The fast component's time constant was 75 ± 5 milliseconds (at 0 millivolts) and it displayed calcium- and voltage-dependent inactivation, whereas the slow component's time constant was 2750 ± 280 milliseconds and it inactivated primarily via voltage. The fast component showed greater steady-state inactivation at holding potentials between -100 and -40 millivolts and had a lower activation threshold than the slow component. The dihydropyridine calcium channel antagonist, nimodipine (0.5 μM) blocked 43 ± 4% of the fast component (from -100 millivolts) but had no effect on the slow component. Higher concentrations of nimodipine (≥1 μM) decreased both components. The amplitude of the slow component was significantly increased by replacing calcium with barium, while the fast component was not changed. The high-threshold component also displayed a ten-fold greater sensitivity to cadmium block than the low-threshold component. The data indicate that mouse β-cells possess at least two distinct calcium currents. Furthermore, the time constant and voltage-dependence of inactivation for the slow component suggest an important role in pacing β-cell burst firing elicited by glucose and other insulin secretagogues.

W-AM-A8

BURSTING ELECTRICAL ACTIVITY IN PANCREATIC BETA CELLS CAUSED BY Ca^{2+}- AND VOLTAGE-INACTIVATED Ca^{2+} CHANNELS.

Joel Keizer and Paul Smolen, Institute of Theoretical Dynamics and Department of Chemistry, University of California, Davis, CA 95616.

Using experimental measurements of Satin and Cook on HIT cells (Pflügers Arch 411, 1 (1989)), we investigate the hypothesis that two classes of Ca^{2+} currents, one that is quickly inactivated by Ca^{2+} and one that is slowly inactivated by voltage, contribute to bursting electrical activity in pancreatic islets. A mathematical model of these currents is fit to the experimental whole cell current-voltage and inactivation profiles, thereby fixing the Ca^{2+} conductance and all activation and inactivation parameters. Incorporating these currents into a model that includes delayed rectifier K^+ channels and ATP-sensitive K^+ channels, our analysis shows that only an abnormal type of bursting can be obtained. Slight modification of activation parameters so as to increase Ca^{2+} channel open times, as suggested by single channel experiments of Ashcroft and Smith, (J. Physiol. (London), 417, 79P (1989)) yields a more robust bursting similar to that observed in intact islets. This reinforces the suggestion that in addition to ATP-sensitive K^+ channels, Ca^{2+} channels may serve as glucose sensors in the β-cell.

W-AM-A9

GLUCOSE AND cAMP STIMULATION OF Ca^{2+} CHANNELS IN INSULIN SECRETING CELLS. Manuel Kukuljan and Illani Atwater. Laboratory of Cell Biology and Genetics, NIDDK, NIH, Bethesda, MD 20892.

Glucose-induced insulin secretion involves Ca^{2+} entry through Ca^{2+} channels. These channels open in response to membrane depolarization resulting from closure of K^+ channels. Direct modulation of L type Ca^{2+} channels by glucose metabolism in mouse β cells has been reported (*Nature* 342:550, 1989). We used the perforated patch technique to study the effect of glucose on whole cell Ca^{2+} currents recorded from rat β cells and HIT cells. 20 mM glucose increased L type current in both cell types. Current increase was more evident (up to 80% of the control in 0 glucose) at Vm between -20 and +30 mV.

Cyclic adenosine monophosphate (cAMP) is increased by glucose in pancreatic β cells and is a potentiator of glucose-induced insulin secretion. In other cell types cAMP dependent phosphorylation of Ca^{2+} channels is an important regulatory mechanism. We studied the effect of the permeable analog 8 Br-cAMP on the electrical activity and Ca^{2+} channels of cultured rat β cells and HIT cells. 1 mM 8 Br-cAMP potentiated glucose induced depolarization and action potential firing of isolated rat β cells. 8 Br-cAMP also evoked a dramatic increase in spontaneous action potential firing in HIT cells. Single Ca^{2+} channel currents were recorded from cell attached patches in HIT cells (bath solution 140 KCl, 10 KHEPES, 1 $MgCl_2$; electrode solution 80 $BaCl_2$, 10 NaHEPES, pH 7.3). 8 Br-cAMP increased the probability of channel openings evoked by depolarizing steps of 60 mV from a holding of -80 mV from < 0.01 to 0.12.

It is suggested that cAMP dependent phosphorylation of Ca^{2+} channels may mediate glucose induced increase of Ca^{2+} currents in insulin secreting cells.

W-AM-B1

TIM BARREL STRUCTURAL MODELS OF PARDAXIN CHANNELS

Gopalan Raghunathan[1], Stewart R. Durell[1], Philip Lazarovici[2] and H. Robert Guy[1];
[1]Lab of Math. Biology, DCBD, NCI, NIH, Bethesda, MD 20892; [2]Dept. Pharmacology & Expt. Ther., School of Pharmacy, The Hebrew Univ., P.O. Box 1172, 91010 Jerusalem, Israel.

Pardaxin is a potent shark repellent made by the Red Sea Moses Sole (Lazarovici, *et al.* In: Hall, S. (Ed.) *Marine Toxins: Origin, Structures, and Pharmacology*. Am. Chem. Soc., 1990; pp. 348-364). It forms voltage dependent membrane channels with only one conductance state. The channel is permeable to inorganic anions and cations and guanidine but not to tris base. The dose-response curve for channel formation suggests that eight to twelve monomers form the channel. Its 33 residue sequence can be divided into three segments, A (GFFALIPKIISS), B (PLFKTLLSAVGSAL) and C (SSSGGQE). Circular dichroism studies indicate both α helical and β strand segments. All models we considered have the following features: (1) residues 5-10 form an α helix positioned on and parallel to the membrane surfaces, (2) segment B forms an amphipathic α helix that spans much of the membrane, (3) the two carboxyls of the C-terminal glutamate form salt bridges with the lysines on segments A and B, (4) all large hydrophobic side chains interact with lipid alkyl chains, (5) the narrow portion of the channel is formed by C segments, and (6) structures are comprised of 8 to 12 monomers. Antiparallel models in which C segments have an extended conformation and form an eight stranded β barrel were calculated to be energetically superior to models in which C segments were given alternative conformations. For parallel models, the C segments must have an extended conformation for the C-terminal glutamates to form salt bridges with the lysines. The parallel models are more consistent with the voltage dependency of channel formation and are similar to the "TIM Barrel" motif that occurs in numerous soluble proteins, in which 8 α helices surround an 8 stranded parallel β barrel. "TIM Barrel" models have been postulated for voltage-gated Na^+, Ca^+, and K^+ channels (Guy & Conti, 1990 *TINS* 13:201) and synexin channels (next abstract).

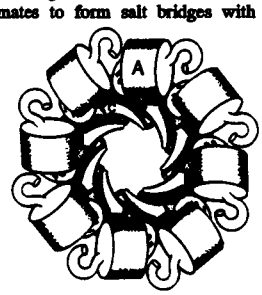

W-AM-B2

A TIM BARREL MODEL FOR SYNEXIN CHANNELS

H.Robert Guy[1], Eduardo M. Rojas[2], A. Lee Burns[2], Eduardo Rojas[2], and Harvey B. Pollard[2]
[1] Lab Mathematical Biology, NCI, NIH, Bethesda, MD 20892;
[2] Lab Cell Biology, NIDDKD, NIH, Bethesda, MD 20892.

Synexin (Annexin VII) is a calcium binding protein, with calcium channel and membrane fusion properties, which has been implicated in the process of exocytosis. Synexin is water soluble in low [Ca^{++}] but aggregates when [Ca^{++}] increases. Like other members of the annexin superfamily, synexin contains four segments that are homologous to each other. Each homologous domain contains five segments (A-E), that we postulate to form α helices. Segments A-D can form amphipathic α helices. The hydrophobic face of each helix is much better conserved among homologous proteins or domains than is the hydrophilic face. These segments are predicted to be helical for most sequences by the Delphi program whereas the intervening segments are not. Segment E is more hydrophobic and the prediction for helix or β strand by Delphi is ambiguious. Intervening segments between A and B (S_1) and between D and E (S_2) are highly conserved and contain negatively charged residues. The model we favor is illustrated below. In this model S_1 and S_2 are β strands that assemble to form an eight stranded parallel β barrel that is surrounded by the more hydrophobic B and E helices. The 'TIM Barrel' spans one monolayer of the membrane. Lipids of the other monolayer are displaced by the more hydrophilic A, C, and D helices which are oriented approximately parallel to the plane of the membrane. A 'TIM Barrel' motif occurs in numerous soluble proteins and has been postulated for other channels (see preceding abstract).

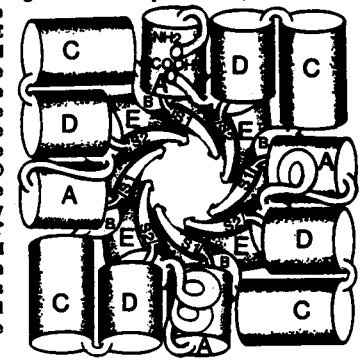

W-AM-B3

MAGAININ CHANNEL: ION SELECTIVITY.

R.A. Cruciani[1], J. L. Barker[1], G. Raghunathan[2], S. Durell[2], R. Guy[2], H-C. Chen[3], and E. Stanley[4]. [1]LNP, NINDS; [2]LMB, DCBD, NCI; [3]ERRB, NICHD and [4]LB, NINDS, NIH. Bethesda MD. 20892. (Spons. J. A. Hammer III).

It was recently observed that the antibiotic peptide magainin 2 and related analogues present cytolytic activity against tumor cells (Cruciani et al. Proc. Soc. Neurosc. (1990) 280.9, abstr.). Utilizing fluorescence techniques we showed that the mechanism of action is related to the ability of the peptides to form cation selective channels on the cell membrane. Now we are presenting data that suggests that these peptides have the same cation selective-channel formation property in artificial lipid bilayers. PS:PE:n-decane bilayers were formed on the tip of a pipet. For all the analogues tested the current trhough the bilayer reversed very close to 0 mV in the presence of symmetrical 100 mM NaCl, but in the presence of asymmetrical gradients of 100:10 mM (cup:bath, cis:trans) it reversed at negative potentials. The reversal potential values in symmetric and asymmetric solutions were as follows: 0 and -31 mV (n=6) for magainin 2; 0 and -34.7 mV (n=7) for magainin A; 0 and -32 mV (n=6) for Z12; 2.3 and -30.3 (n=7) for magainin G; 0 and -31 mV for magainin 1, respectively. The cation selectivity criteria was fullfilled by a model in which the lining of the channel is formed exclusively of lipid head groups. In this model the role of the magainin is to stabilize the orientation of the channel lining groups by covering their alkyl chains on the membrane surfaces. We favor channels that have six-fold symmetry because they allow the magainin lipid complex to form a two-dimensional hexagonal array in which all magainin molecules have the same conformation and are exposed to the same environment. In the present model we consider residues 2-17 to be helical. All the head groups that line the channel are assumed to be PE and all those on the surface that interact with magainin are assumed to be PS. The model pores are lined by 72 PE head groups. The electric field inside these channels was calculated to be electronegative. Negatively charged groups at the C-termini of magainins are near the entrances of the channel and contribute to the electronegativity.

W-AM-B4

MODELING the CHANNEL STRUCTURE of CECROPIN

Stewart R. Durell, Gopalan Raghunathan, & H. Robert Guy;
Lab. Math. Biol., DCBD, NCI, NIH, Bethesda, MD 20892.

Cecropins and sarcotoxins are small, homologous, antimicrobial peptides produced by some insects. Cecropins form voltage dependent channels in lipid bilayers (Cristensen et al.; 1988 PNAS 85:5072). The N-terminal portion (res. 1-22) of cecropin forms an amphipathic helix with a narrow hydrophobic face. This segment is followed by the helix disrupting gly-pro sequence. The remaining C-terminal portion forms a more hydrophobic amphipathic helix (res. 25-37), with a narrow hydrophilic face. The N-terminal helix exhibits a pattern called unilateral conservation, in which one helical face is highly conserved among homologous peptides, and the opposite face is poorly conserved. The pattern is unusual in that it does not correspond to the hydrophilic and hydrophobic faces but rather to an interface region. Using the assumption that conserved patches of the topology are structurally important, two cecropin strands were arranged as an antiparallel dimer so that the conserved faces are in contact, and salt bridges occur between conserved side chains. The N-terminal helices are envisioned to lie parallel to the membrane plane and sink down between the lipid head-groups. Hydrophobic residues on the bottom side of the dimer are in contact with the aliphatic phase of the membrane, and hydrophilic residues on the top side of the dimer are in contact with the polar head-groups and solvent. The C-terminal segments of the dimer are bent down perpendicular to the membrane plane, extending through the second lipid monolayer. The insertion of the C-terminal segments through the membrane could be the voltage dependent step in channel formation. In the model we currently favor, multiple cecropin dimers aggregate to form a hexagonal lattice, and the C-terminal segments meet in the regions of six-fold symmetry to form the pores, as illustrated in the figure (α carbon trace, looking down at the membrane plane).

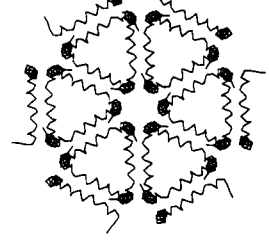

W-AM-B5

SECRETORY VESICLE SPECIFIC ION PERMEABLE CHANNELS FROM THE NEUROHYPOPHYSIS. Keith E. Krebs and Gerald Ehrenstein. Lab. of Biophysics, NINDS, NIH, Bethesda, MD 20892

Recently, Navone et al. (J.Cell Biol. 109, 3425, 1989) have demonstrated that two distinct populations of secretory vesicles are present in the bovine neurohypophysis; 100-300 nm diameter neurosecretory granules (NSG) that contain peptide neurohormones, and 40-60 nm microvesicles (MV) of unknown function that are biochemically related to small synaptic vesicles of presynaptic nerve terminals. We now report that these two classes of neurohypophysis vesicle appear to possess distinct ion permeable channels. NSG and MV from bovine neurohypophysis were prepared as described by Navone et al. with the added final step of vesicle separation on a 160 x 1.5 cm, 3000 Å controlled pore glass bead column, to yield highly purified vesicle preparations on the basis of size. NSG eluted from the column at 1.05-1.25 x V_0 and MV eluted at 1.5-1.8 x V_0. Purified NSG or MV were added to the cis side of painted lipid bilayers (80% PE/ 20% PC). Fusion of NSG with the bilayer usually resulted in the incorporation of a chloride-permeable channel of high conductance (>150 pS) which was dependent on calcium (peak open probability of 80% at 200-300 nM Ca^{2+}) and was blocked with DIDS. In contrast, the fusion of MV with the bilayer resulted exclusively in the incorporation of a potassium-permeable channel with conductance >100 pS, that does not appear to be calcium-dependent. Occasionally the fusion of NSG with the bilayer resulted in the incorporation of a potassium-permeable channel that appeared to be similar to the MV channel, and it is not clear whether this represents a channel present in the membrane of NSG, or is the result of MV contamination of the NSG preparation.

W-AM-B6

CHLORIDE CHANNEL ACTIVITY REGULATES SEROTONIN RELEASE IN RAT MUCOSAL MAST CELLS. Chr. Romanin, M. Reinsprecht, I. Pecht*, H. Schindler. Inst. f. Biophysics, Univ. of Linz, A-4040 Linz, Austria; * Department of Chemical Immunology, The Weizmann Institute of Science, Rehovot 76100 Israel.

Crosslinking of IgE-carrying receptors ($Fc_\epsilon RI$) at the surface of basophils or mast cells by the corresponding polyvalent ligand (i. e. antigen) initiates a cascade of cellular processes culminating in secretion of inflammatory mediators (e. g. histamin and serotonin). In the present study we correlated the release of serotonin with changes in membrane permeability. Crosslinking of $Fc_\epsilon RI$ in rat basophilic leukemia cells (RBL-2H3) resulted in the induction of a Cl^- ion current with a unitary conductance of 32 pS. Gating of this current was voltage dependent, exhibiting higher open probabilities at depolarized voltages. This antigen-induced current was inhibited by the Cl^- channel blocker 5-nitro-2-(3-phenylpropylamino) benzoic acid (IC_{50}=52±21 μM). The dose response for this inhibition correlated well with the inhibition of serotonin release (IC_{50}=77±60 μM). Taken together, our findings indicate a functional role of Cl^- current in mediator secretion from mucosal mast cells. (supported by the Austrian Res. Funds, project S-45/03)

W-AM-B7

THE INPUT RESISTANCE OF CEREBELLAR PURKINJE CELLS MEASURED WITH TIGHT-SEAL PATCH PIPETTES.
M. M. Usowicz, M. Sugimori, R. Llinás, Dept. of Physiology and Biophysics, New York University Medical Center, New York 10016

Estimates of the input resistance (R_{in}) of mammalian central neurons calculated from tight-seal whole-cell recordings are higher than those obtained with intracellular microelectrodes (ME). For instance, values for R_{in} of cerebellar Purkinje cells (PC) are 500 MΩ for dissociated PC in whole-cell voltage clamp (Hirano & Ohmori, PNAS 83:1945), 40 MΩ for PC in organotypic slice cultures recorded with ME (Kapoor et al, Neuroscience 26:493), and 15 MΩ for PC in a cerebellar slice recorded with ME (Llinás & Sugimori, J.Physiol 305:171). The lower values are thought to reflect a ME impalement leakage (Hamill et al, Pflügers Archiv 391:85). However, ME impalement does not modify the membrane potential or the threshold for spike initiation in the manner expected from the presence of such large leak conductance. In order to examine this issue, whole-cell recordings were made from *adult* PC in thin cerebellar slices of the guinea pig (Edwards et al, Pflügers Archiv 414:600), with patch-pipettes containing (in mM) 135 KCl, 10 K_2-EGTA, 10 Na-HEPES, pH 7.2 with KOH (resistance ≤5MΩ). Recordings were made at 22° C from PC in voltage clamp and current clamp modes with a patch-clamp amplifier, and in current clamp mode with an high-input impedance bridge amplifier, of the type previously used in our laboratory for ME recordings. A relay was used to switch between the two amplifiers during recording from a single neuron.

The three recording modes yielded similar values for R_{in} of 50-90MΩ. These values are somewhat higher than those measured with ME for adult PC in slices or organotypic culture. However, our measurements of the resting potential for PC in slices (-60mV) and firing threshold (about 10mV from resting potential) obtained with patch pipettes, are similar to those of PC in slices or organotypic culture, obtained with ME. The differences in R_{in} may be due to the different temperature at which measurements were made, since temperature determines background activity and cell biochemistry (22° C, this study; 37° C, for ME recordings). On the other hand, all our measurements are lower than R_{in} of dissociated PC. This difference probably reflects the smaller size and reduced number of synaptic inputs of dissociated neurons, compared with adult neurons in slices or organotypic culture. Our findings indicate that the differences reported for the use of ME and patch-pipettes to measure R_{in} may not be as significant as initially thought.

W-AM-B8

HYDROGEN ION CURRENTS IN RAT ALVEOLAR EPITHELIAL CELLS. **by Thomas E. DeCoursey, Department of Physiology, Rush Medical Center, Chicago, IL.**

Large H^+ currents (hundreds of *pA*) were observed in cultured alveolar epithelial cells studied with the whole-cell patch-clamp technique. Potassium and chloride conductances were eliminated by using impermeant N-methyl-D-glucamine and methanesulfonate in both external and internal solutions. In most experiments the pipette solution was buffered to *pH* 5.5 with 5 *mM* MES. H^+ currents activate slowly on depolarization, and deactivate upon repolarization with a time constant of tens to hundreds of msec, being faster at more negative potentials. Regardless of external *pH*, H^+ currents are mainly outward. The reversal potential, V_{rev}, determined from tail currents changed with external *pH* in a manner roughly consistent with the H^+ gradient, supporting H-selectivity.

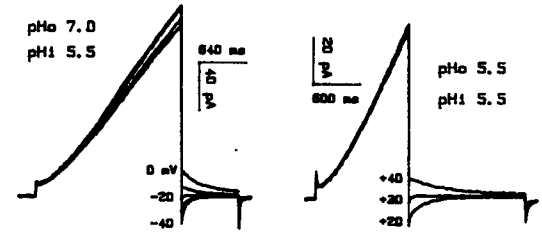

Absolute values of V_{rev} and several other results indicate that $[H^+]_i$ deviates from $[H^+]_{pipette}$ in the whole-cell configuration. Generally resembling H^+ currents in snail neurons (Thomas & Meech, 1982, *Nature* 289:826; Byerly *et al*, 1984, *J.Physiol.* 351:199) and *Ambystoma* oocytes (Barish & Baud, 1984, *J.Physiol.* 352:243), those in alveolar epithelium are inhibited by Zn^{++} or Cd^{++} at 10–100 μM.

Supported by NIH grants HL01928 & HL37500.

W-AM-B9

ADP, BUT NOT THROMBIN, RAPIDLY ACTIVATES CATION CHANNELS IN HUMAN PLATELETS. M.P.Mahaut-Smith*, S.O.Sage# and T.J.Rink$. *Howard Hughes Medical Institute M-047, UCSD, La Jolla, San Diego, CA 92093; #Physiological Laboratory, Downing Street, Cambridge, U.K. and $Amylin Corporation, 9373 Towne Center Drive, Suite 250, San Diego CA 92121.

We have used the nystatin perforated patch technique (Horn & Marty, 1987; J.Gen.Physiol. 92, 145-159) to study agonist-evoked currents in "whole-cell" recordings from human platelets. Platelets were prepared as previously described (Mahaut-Smith et al., 1990, J.Biol.Chem., 265,10479-10483). Patch pipettes were filled with (in mM) 140 KCl, 1 $MgCl_2$, 1 EGTA, 10 HEPES, 10 glucose, pH 7.4 plus 50-100μM nystatin. The bathing medium contained (in mM) 145 NaCl, 5 KCl, 1 $MgCl_2$, 10 HEPES, pH 7.4. Agonists were applied from a "puffer" pipette, while the potential was clamped near its resting value. At -70mV, 1 unit/ml thrombin had no effect (n=6), whereas ADP activated a transient inward current within 40 ms. The current reached a peak (13-31 pA, range from 5 cells) within a further 40ms, then decayed exponentially (tau = 107-189 ms, range from 5 cells) even in the continued presence of ADP. Single ADP-evoked channel currents could also be resolved; the unitary current at -70mV was 0.9 ± pA (n=8). Channel activation by ADP was independent of voltage within the range tested (-110 to -40mV). E_{rev} for the ADP channel was estimated by extrapolation of the single channel current-voltage relationship and was close to 0mV in both normal saline and a low Cl^- saline and approximately -13 mV in 110mM $BaCl_2$ saline. This indicates that the channel is equally permeable to Na^+, K^+, Ba^{2+} and presumably also Ca^{2+}. The time course of the ADP-evoked current is similar to the rapid phase of Ca^{2+} and Ba^{2+} entry in stopped flow fluorescence studies (Mahaut-Smith et al, 1990, J.Biol.Chem. 265, 10479-10483).

Supported in part by research donation from Smith Kline & French; S.O.S. is a 1983 Royal Society University Research Fellow.

W-AM-C1

LOW LEVEL COMPRESSION OF RABBIT PSOAS FIBERS BY DEXTRAN T-500 DECREASES THE RATE OF REVERSE POWER STROKE, AND THE HIGH LEVEL COMPRESSION DECREASES THE RATE OF POWER STROKE. Yan Zhao and Masataka Kawai. Department of Anatomy, The University of Iowa, Iowa City, IA 52242.

The actin-myosin lattice spacing of chemically skinned rabbit psoas fibers was osmotically compressed by dextran T-500, and the effects of MgATP and phosphate (Pi) ions were studied on exponential processes (B) and (C) with the sinusoidal analysis technique at fixed dextran concentrations. Our earlier results indicate that the process (C) characterizes the cross-bridge detachment step, and the processes (B) characterizes the power stroke step that occurs on the conformational change (AMDP $\longrightarrow$ AM*DP; A=actin, M=myosin, D=MgADP) and that precedes the Pi release step (Kawai and Halvorson, Biophys. J. in press). Experiments were performed at 20°C in the presence of (mM:) 6 CaEGTA (pCa 4.82), 5 free ATP, 0-10 MgATP, 0-16 Pi, 10 MOPS (pH 7.00), 15 phosphocreatine, 160 units/ml creatine kinase, and the ionic strength adjusted to 200mM by K propionate. The lattice spacing was estimated from the width of the fibers measured under a high power-light microscope. At a low level compression (0-15%) by 0-6.3% dextran, the rate constant of the reverse power stroke step decreased, and isometric tension increased to 123%. At a high level compression (19-24%) by 9-11.7% dextran, the rate constant of the power stroke step decreased, and isometric tension changed to 121-102%. Evidently, the myosin heads have an increased difficulty in performing the power stroke at the high level compression. In both cases, the decreases in the rate constants were consistent with the changes in isometric tension. The association constant of Pi to the cross-bridges in the AMD* state, and that of MgATP to the AM state were little affected by the compression. The compression had smaller effects on the detachment step of cross-bridges. Our results demonstrate the significance of the actin-myosin lattice spacing in promoting the power stroke reaction and its reverse reaction in fast twitch skeletal muscle fibers.

W-AM-C2

FLIGHT MUSCLE FROM DROSOPHILA TROPOMYOSIN MUTANT TRAPPED IN RELAXED STATE. **J.E. Molloy & D.W. Maughan, Dept. Physiology & Biophysics, Univ. of Vermont, Burlington, VT 05405 USA**

In Drosophila, tropomyosin (Tm) is encoded by two genes (TmI,II) which produce six protein products by alternative splicing. Here we report results of studies on asynchronous flight muscle fibers (IFM) of the flightless genetic mutant Ifm(3)3 in which a TmI IFM specific isoform is absent (Karlik & Fyrberg, 1985, Cell 41: 57). Myofibrils exhibit a core of normal lattice and a periphery of disorganized lattice. Myofibrillar bundles bathed in ATP-salt solution exhibit relaxed levels of stiffness, force, and ATPase that remain essentially unchanged in the presence of Ca^{2+}; stretch activation is undetectable. However, removal of ATP from the bathing solution produces the usual rigor state (below). Flight in Ifm(3)3 has been rescued by P-element transfection of the TmI gene (Tansey et al., 1987, EMBO 6:1375), and mechanical tests of IFM from these flies (P[10-2]/Ifm(3)3) show wild type responses. Together, these results suggest that a deficiency of the IFM specific form of Tm produces muscles that are trapped in a relaxed state, leading to the flightless phenotype. In summary, actomyosin interactions are blocked, even in the presence of Ca^{2+}. With removal of ATP, actomyosin interactions are strong enough to overcome steric hindrance.

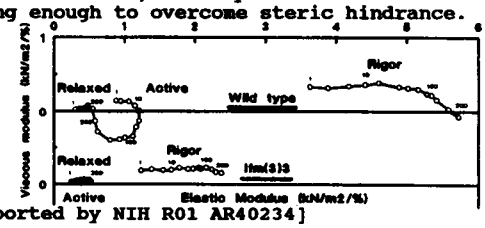

[Supported by NIH R01 AR40234]

W-AM-C3

ALTERATION OF CROSSBRIDGE KINETICS BY AN ACTIN MUTATION. M Peckham, M A Ferenczi & D C$_8$S White. Biology Dept, University of York, York, UK. N.I.M.R. London, NW7 1AA, U.K.

A genetically engineered mutation in the actin expressed in the indirect flight muscles (IFM) of Drosophila melanogaster has recently been reported to alter the mechanics of active demembranated fibres from the IFM compared to wild type (Drummond et al, 1990, Nature, in press). The mutation (G368E) causes a single amino acid change from glycine to glutamic acid at position 368 (close to the COOH terminus). The rate constant for the delayed tension increase following a rapid stretch of active muscle fibres is reduced by about 30% compared to wild type, and active tension and stiffness are higher (Drummond et al, as above). The decreased rate constant could be caused by an increased stiffness of the active crossbridges when attached to actin, or by a reduction in one of the rate constants of the actomyosin ATPase. Rapid release of ATP by photolysis of caged-ATP in rigor IFM fibres in the absence of Ca^{2+} caused relaxation. The latter part of the relaxation was approximated to an exponential with a rate constant of 40.3 $\pm$ 1.1$_1$ s^{-1} (mean $\pm$ S.E.) for 3 wild type fibres and 27.5 $\pm$ 3.2 s^{-1} for 3 G368E fibres (see Fig 1). X-ray diffraction of active IFM fibres did not show any differences in the equatorial reflections. The reduction in rate constant for the delayed tension increase is more likely to be due to a reduction in one of the rate constants of the actomyosin ATPase.

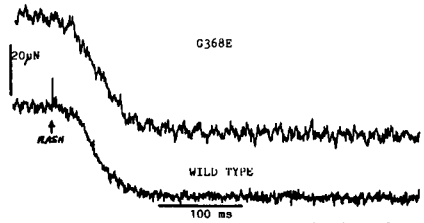

Fig 1. Time course of tension following ATP release from caged-ATP from rigor, 5mM caged-ATP, 15°C, 0.15M ionic strength.

W-AM-C4

WEAK CROSS-BRIDGE BINDING IS ESSENTIAL FOR FORCE GENERATION. EVIDENCE AT NEAR PHYSIOLOGICAL CONDITIONS. Th. Kraft*, J.M. Chalovich#, L.C. Yu+, B. Brenner*;
*University of Ulm; #East Carolina Univ.; +NIAMS, NIH.

Myosin cross-bridges have been shown to be able to attach to actin even under relaxing conditions in solution (Chalovich et al., JBC, 1981, p. 575) and in chemically skinned rabbit psoas fibres (Brenner et al., PNAS, 1082, p. 7288). The functional significance of this weak cross-bridge binding has been controversial. Recently (Brenner et al., Biophys. J. 57, 397a, 1990), we have used the protein caldesmon and its inhibitory polypeptide fragments as probes for the weak cross-bridge binding in single rabbit psoas fibres, since caldesmon inhibits weak cross-bridge binding in solution. We showed that at low temperature and low ionic strength caldesmon and its actin binding polypeptide fragments decrease stiffness under relaxing conditions and inhibit force generation. Using the actin binding caldesmon polypeptides, we have continued studying the weak cross-bridge binding at temperatures up to 20°C and ionic strengths as high as 170 mM, both in the absence of Ca^{++} (MgATP and MgATPγS as nucleotides) and at pCa of about 4.5 (with MgATPγS as nucleotide). Our data indicate that (i) even under near physiological conditions weak cross-bridge attachment occurs in muscle fibres to a significant extent, and (2) inhibition of weak cross-bridge attachment by caldesmon, without inhibition of strong cross-bridge binding is, under all conditions studied, sufficient to inhibit active force. This suggest that weak cross-bridge attachment is essential for the production of active force.

W-AM-C5

PROBING FOR SITES INVOLVED IN WEAK AND STRONG CROSS-BRIDGE BINDING TO ACTIN BY MYOSIN PEPTIDES. Th. Kraft*, I. P. Trayer+, B. Brenner*, * University of Ulm, FRG; +University of Birmingham, UK.

Based on biochemical and skinned fiber studies it was proposed that during active contraction myosin cross-bridges cycle between two major configurations, a weak- and a strong-binding configuration. X-ray diffraction studies and electron microscopy suggested that the mode of weak attachment is different from the strong cross-bridge attachment, possibly due to differences in the actomyosin interface for weak and strong attachment. To test this idea we used short synthetic peptides (up to 10 amino acids) of the myosin heavy chain to see whether such peptides can specifically compete with either type of binding. Of the various peptides used, one was found which specifically inhibited active force without affecting the weak cross-bridge binding (up to 300μM of the peptide, producing >50% inhibition of active force). Furthermore, the contractile system was "activated" by addition of this peptide (leftward shift of the force pCa relation). At concentrations >300μM the leftward shift resulted in partial activation even under relaxing conditions. The peptide represents a sequence around the SH1 group, but is different from the peptide of Suzuki et al. (JBC, 262 11410, 1987) which was recently shown to not specifically affect cross-bridge interaction with actin (Chase and Kushmerick, Biophys. J. 57, 538a, 1990). Adjacent and other sequences were at least an order of magnitude less effective. These data are consistent with the idea that at least part of the actomyosin interface involved in the strong cross-bridge interaction is not involved in the weak interaction. Further studies have to show whether the peptide activates the contractile system by the same mechanism as strongly attached cross-bridges.

W-AM-C6

SARCOMERE SHORTENING PER ATP MOLECULE RELEASED FROM CAGED ATP WITHIN RABBIT SKINNED MUSCLE FIBERS. Hideo Higuchi and Yale E. Goldman, Dept. of Physiol. and Penna. Muscle Inst., Univ. of Pennsylvania, Philadelphia, PA 19104

To obtain the filament sliding distance (D_s) per molecule of ATP hydrolyzed by actomyosin we measured isotonic shortening after limited release of ATP by laser photolysis of caged ATP in glycerol-extracted single fibers from rabbit psoas muscle. The fibers were loaded with caged ATP in the presence of 30 μM Ca^{2+} and then immersed in paraffin oil, so that ATP would be liberated only within the fibers. Just after photolysis, the tension was clamped to a preset value and the fibers shortened isotonically at 20 °C from 2.8 μm sarcomere length until either the ATP was exhausted or sarcomere length reached 2.2 μm. Total shortening (D_t) per mM of released ATP averaged 560, 430, 350 nm per half sarcomere at tensions ~7, ~26 and ~44% of isometric tension (P_o) respectively (figure). 500 Hz stiffness (S) averaged 64, 67 and 72% of the 2.8 μm rigor stiffness during isotonic shortening at the corresponding tensions. Assuming that at 2.8 μm, 105 μmoles ($[M_o]$) of myosin heads are in the overlap region per liter fiber volume, sliding distances were calculated as $D_s = D_t \times S \times [M_o]$. D_s averaged 38, 30 and 24 nm at 7, 26 and 44% P_o. The results suggest that at low loads, for each ATP molecule utilized, a myosin head interacts with the thin filament for a distance greater than S-1's length. Supported by the MDA and NIH grant AR26846.

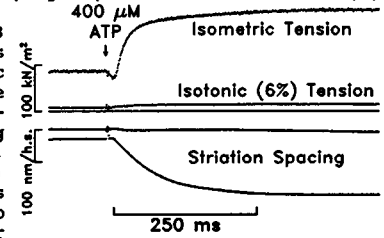

W-AM-C7

CHARGE-DEPENDENT INHIBITION OF ACTOMYOSIN INTERACTION IN RABBIT PSOAS MUSCLE FIBERS BY MYOSIN HEAVY CHAIN PEPTIDES. P.B. Chase, T.W. Beck, & M.J. Kushmerick, Depts. of Radiology and Physiology & Biophysics, Univ. of Washington, Seattle, WA 98195

Peptides of 3 to 28 residues, derived from the primary sequence of vertebrate skeletal myosin heavy chain (MHC) around SH_1 (Cys 707), have been reported to inhibit the interaction of myosin and actin competitively by binding to actin and mimicking the actin-binding function of myosin (Suzuki *et al.*, 1987, *JBC* **262**:11410; Chase & Kushmerick, 1988, *JCB* **107**:258a; Chase & Kushmerick, 1989, *Biophys. J.* **55**:406a; Suzuki *et al.*, 1990, *JBC* **265**:4939; Keane *et al.*, 1990, *Nature* **344**:265). We found that inhibition of maximum Ca-activated force of skinned fibers was not a unique property of the native primary sequence when amino acid variations were made which altered the structure but not the net charge (3+) of the peptide (Chase *et al.*, 1990, *Biophys. J.* **57**:538a). Compared with the native sequence peptide (IRICRKG, $K_{0.5}$ ~ 3 mM), peptide IRICRKG-NH_2, with a net charge of 4+, was a more effective inhibitor of force ($K_{0.5}$ ~ 2 mM) while peptide IEICRKG, with a net charge of 1+, was a less effective inhibitor of force ($K_{0.5}$ ~ 5 mM). The peptide's (IRICRKG) contribution to ionic strength (μ) of the solution was not responsible for the inhibition because lowering μ from 200 mM to 150 or 100 mM did not increase the relative efficacy of the peptide. In summary, inhibition of maximum Ca-activated force by peptides from the SH_1 region of MHC depended on the net charge of the peptide rather than on the specific sequence of amino acids. Supported by NIH grant HL31962.

W-AM-C8

TENSION RESPONSES TO RAPID LENGTH CHANGES IN INTACT CELLS ISOLATED FROM FROG HEART. By G. Cecchi, F. Colomo, C. Poggesi and C. Tesi, from Dipartimento di Scienze Fisiologiche, Viale Morgagni 63, I-50134, Firenze, Italy.

The cells were held horizontal in a trough of 1 mM Ca^{2+} Ringer solution at 21 °C between two sucking micropipettes. One of them acted as a cantilever force probe (compliance 10-20 nm/nN; frequency response in Ringer solution 600-800 Hz). The other sucking pipette was stiff. Tension was measured at one cell end by photoelectrically recording the elastic deflection of the force probe tip. The cell shortening during an ordinary twitch contraction was about 1% of the resting cell length (lo). Rapid length changes of varying size, complete in less than 2 ms, were imposed to the other end of the cell by means of a loudspeaker coil motor holding the stiff micropipette. In the figure the effects of a rapid shortening applied to a ventricular cell just before stimulation or before the peak of the twitch are compared. It is of interest to note that a step shortening of 2% lo is required to drop the peak twitch tension to zero. By taking into account the deflection of the force probe at the time of the release (0.9 % lo in this case), the effective shortening required to drop tension to zero is 1.1 % lo, a value 5-10 times smaller than in multicellular cardiac preparation.

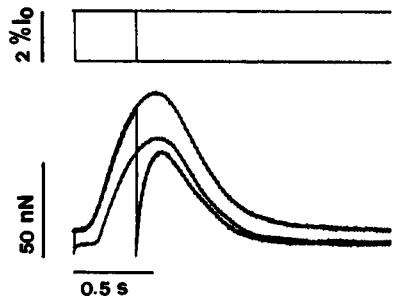

W-AM-C9

CONTRIBUTION OF DAMPED SERIES ELASTIC ELEMENT RECOIL TO THE MEASURED SHORTENING VELOCITY OF SKINNED FIBERS

C. Y. Seow and L. E. Ford, Department of Medicine, The University of Chicago, Chicago, IL 60637

Maximum shortening velocities of skinned fibers from rabbit psoas and sheep extensor digitorum longus muscles were measured at 1-2 °C by the slack test and by extrapolating force-velocity curves to zero load. Both overall muscle velocity and sarcomere velocity were measured with each method. Maximum velocity assessed from the force-velocity curves (1.07 $\mu m \cdot s^{-1} \cdot$ half-sarc^{-1} ±0.12 SD, rabbit; 0.47±0.08, sheep) was not significant-ly different from sarcomere velocity measured by slack test ($p>.1$). Maximum overall muscle velocity measured from the slack test was significantly ($p<.001$) and substantially (about 60%) greater than maximum sarcomere velocity. The difference is attributed to damped recoil of the series elastic elements. Overall muscle velocity was substantially greater than sarcomere velocity during the early phases of isotonic shortening, particularly at low loads. This rapid shortening obscured velocity transients that were plainly obvious in the sarcomere length records. Isotonic velocities were measured after these transients had ended, when sarcomere and overall muscle velocity were the same. A large difference between overall muscle length change and sarcomere length change (about 6% muscle length at low loads) was diminished by about half during the isotonic step and the remaining half declined at a diminishing rate over 20-30 ms. This result, which is explained by about half of the series elastic element behaving as a viscoelastic element, can account for the greater maximum velocity that is frequently found with the slack test.

(Supported by USPHS Grant HL44398 and a MRC of Canada Fellowship).

W-AM-D1

THREE DIMENSIONAL IMAGING USING MULTIPLY SCATTERED NEAR INFRARED LIGHT. John Haselgrove*, Jack Leigh+, Britton Chance+, Conway Yee@, and Gabor Herman@. Departments of *Biochemistry, Dental School, +Biochemistry, Medical School, @Radiology, University of Pennsylvania, PA.

Near infrared light (NIR) has been shown to be suitable for recording the oxygenation status of tissue. We are investigating the use of time of flight measurements to image the distribution of absorption coefficients in an inhomogeneous three-dimensional medium (such as a human brain). NIR light injected at one point into human head, (or a phantom simulating the head) is detected at 15 points around the object. Despite the fact that the light is scattered with a mean scattering length of << 1mm, and a migration path length of 28 cm, over which a significant number of photons travel. We are performing three dimensional Monte Carlo simulations of the probable paths of these photons injected into a three dimensional object; a cylinder. We have calculated the probability that a photon will pass each voxel during the migration from emitter to detector. When the medium in the cylinder is homogeneous, the mean path from emitter to detector is in general not a straight line but is curved towards the center of the volume. The presence of an absorber in one of the paths does not merely decrease the intensity of the light reaching the detector, but alters the probable path as shown by the simulations in 620 model to be accurate to 120% of the diameter of an absorber that is 20% of the model diameter. It is be possible to detect such changes in mean path length using phase modulated spectroscopy to an accuracy of <5 mm (Gratton, E. in preparation). Our calculations also simulate the time course with which photons arrive at the detector, permitting us to utilize time of flight spectroscopic measurements too.

W-AM-D2

CORRELATION OF TIME AND AND FREQUENCY DOMAIN MEASUREMENTS OF HEMOGLOBIN ABSORBANCE CHANGES IN TISSUE MODELS. B. Chance and E.M. Sevick, Dept. Biochem/Biophys, Univ. of Pennsylvania, Phila, PA 19104

The use of time resolved spectroscopy to quantitate concentrations in a highly scattering medium such as tissue has been described previously (Chance, et al (1990) Biophys.J.55:451). Time resolved spectra (TRS) give complete information about the kinetics of photon migration, by directly measuring the time distribution of photon pathlengths and are here compared with frequency domain measurements to provide a simpler method to quantitate hemoglobin concentration in tissues.

The phase-shift of 220 MHz modulated light and the distribution of photon pathlengths using time resolved spectroscopy at 760 nm are compared in a model system of hemoglobin and yeast (Fig.1). The small diagrams indicate that time domain method exhibits an exponential decay rate which is linearly dependent upon the concentration, whilst phase modulation (PMS) plots directly the phase shift caused by the pathlength changes due to hemoglobin deoxygenation. Fig.2 plots a correlation of these two measures for a series of hemoglobin concentrations and for 9 cm input/output separations. A satisfactory agreement between the two methods justifies quantitative studies in the frequency domain (Sevick, these abstracts).

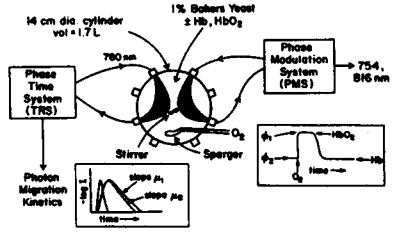

Fig. 1. Correlation of TRS and PMS in a yeast/hemoglobin brain model

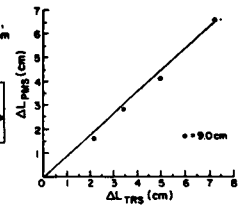

Fig. 2. Correlation of path length changes measured by TRS and PMS.

SUPPORT: NIH CA 08783 (EMS) and HL 44125, NS27346, NS-22881

W-AM-D3

ATOMIC FORCE MICROSCOPY OF PURPLE MEMBRANES. D.L. Worcester, Biology Division, University of Missouri, Columbia, MO 65211. H.S. Kim, R.G. Miller and P.J. Bryant, Physics Dept. University of Missouri-Kansas City, Kansas City, MO 64110.

The surfaces of purple membranes from *Halobacterium halobium* have been imaged using atomic force probes mounted in a scanning tunneling microscope. The atomic force images show the circular trimers of bacteriorhodopsin which are about 5nm diameter. Finer details of the protein surface structure in the images are not readily discerned but are indicated in Fourier transforms of the images. Many of the images show parallel rows separated by the spacing corresponding to the lattice constant from diffraction methods, but do not show distinct trigonal arrangement of the protein trimers. This suggests that the atomic force probes often have anisotropic resolution functions which depend on the orientation of the lattice with respect to the scan direction.

The membranes samples were prepared for imaging as a stack of many membranes fixed to a mica base so that the immediate substrate under the membrane imaged was another membrane. This helped to minimize artifacts due to substrate imaging. The membranes were imaged in air with ambient humidity in the range 50-60%r.h., for which there is at least a monolayer of water on the membrane surface. This hydration layer is apparently important to the smooth operation of the atomic force probe and for avoiding damage to the membrane due to the contact force and frictional forces. For the latter, scan rate is also important. Different types of atomic force probes have been developed and tested during this work. They are described together with their relative performance.

W-AM-D4

CONFOCAL RATIOMETRIC Ca^{2+} IMAGES MEASURED USING FURA-2 AND A CONVENTIONAL EPIFLUORESCENCE MICROSCOPE. J.R. Monck, A. Oberhauser, T. Keating and J.M. Fernandez, Dept. of Phys. and Biophys., Mayo Clinic, Rochester, MN 55905.

The cytosolic free Ca^{2+} concentration is important in the regulation of many biological processes including muscle contraction and secretion. The introduction of the ratiometric Ca^{2+} indicator dyes, fura-2 and indo-1, and advances in digital imaging and computer technology has made it possible to detect Ca^{2+} changes in single cells with high temporal and spatial resolution. However, the detection of localized Ca^{2+} concentrations using a conventional epifluorescence microscope is limited because the true image is distorted by the microscope light path (principally by the objective) so that light emanating from an ideal point source becomes spread out and takes on a characteristic shape, the point spread function. Thus, the observed image is impaired by blurring of the in-focus image plane and contamination with out-of-focus information. One solution to this problem is to use a confocal microscope which only detects in-focus information, but this approach has several disadvantages for low light fluorescence measurements in living cells. An alternative approach is to remove the out-of-focus information. The "nearest neighbor deblurring" scheme (Agard, 1984) uses digital image processing in the Fourier domain to produce confocal in-focus images that are used for 3-dimensional reconstructions. We have used a modification of this scheme, a "pseudo-nearest neighbor deblurring" method, to deblur images of fura-2 loaded mast cells from beige mice and generate confocal ratiometric intracellular Ca^{2+} images with high spatial resolution. The confocal properties of these images are demonstrated by taking pairs of images at different focal planes 0.5 μm apart. Adjacent images show distinct changes in the size and shape of secretory granules, which exclude the indicator and appear in-focus in all sections. With this technique, we can observe Ca^{2+} transients in narrow regions of cytosol between the secretory granules and plasma membrane that can be less than 0.5 μm wide. Moreover, these Ca^{2+} increases can be seen to coincide with the swelling of the secretory granules that follows exocytotic fusion.

W-AM-D5

IMAGING OF PHOTOSENSITIZED SUBCELLULAR TARGETING.
M. Scholz, B. Goff, R. Bachor, T. Hasan. Wellman Laboratories of Photomedicine, Massachusetts General Hospital, Harvard Medical School, Boston, MA 02114

Photodynamic therapy (PDT) is a relatively new experimental method for the treatment of cancer. In this modality, nontoxic compounds (photosensitizers, PS) are taken up by malignant tissue and activated by light to form cytotoxic species resulting in cell death. A major advantage of this approach is its inherent dual selectivity due to PS localization in target tissue and control of illumination site(s). Target-cell specificity may be further improved by the coupling of PS to molecular delivery systems. Coupling of PS to macromolecules can profoundly affect the efficiency, site(s) and mechanism(s) of uptake. In this study, we have investigated photochemical targeting at a subcellular level using efficient PS, Chlorin e6 (Ce_6), free and conjugated, to three delivery systems: polyglutamic acid (PGA); OC125, a monoclonal antibody (Mab) directed against human ovarian cancer antigenes; and latex microspheres (MS). Because PS have inherent fluorescence, no additional staining is necessary; however, generally the fluorescence quantum yield of PS are much lower than the usual fluorescent stains such as fluorescein and rhodamin. The localization of PS' fluorescence in single living cells at therapeutically relevant concentrations, was imaged by the complementary techniques of video-microscopy using a silicon intensified targeted camera (SIT) and by a confocal laser scanning microscope (CLSM). The CLSM provided the higher three-dimensional resolution, while SIT microscopy provided the advantage of light source flexibility. Our initial results using ovarian and bladder cancer cells show different mechanisms of uptake for the free and bound PS at low concentrations relevant for PDT. Free Ce_6 bound largely to membrane structures, while Ce_6 conjugated to MS appeared to localize in lysosomes. Mabs bound to Ce_6 showed largely plasma membrane localization, while PGA-Ce_6 was internalized effectively. These data and extended studies on the time course and relative quantification of these uptake mechanisms will be discussed.

W-AM-D6

PROTON DECOUPLED ^{31}P 3-D CSI SPECTRA FROM THE HUMAN BRAIN
T.R. Brown,[1] J. Murphy-Boesch, D. Vigneron[2], S.J., Nelson[2], J.S. Taylor[1]
Fox Chase Cancer Center, Philadelphia, PA 19111, [1]St. Jude Children's Research Hospital, Memphis, TN 38101, [2]University of California, San Francisco, CA 94143

In order to enhance our NMR techniques for assessing the concentration and 3D distribution of ^{31}P metabolites we have designed and constructed a novel dual-tuned $^{1}H/^{31}P$ quadrature transmit/receive birdcage for human brain studies. This has enabled us to acquire proton decoupled ^{31}P NMR spectra from the human brain with improved sensitivity and spectral resolution capable of resolving phosphocholine from phosphoethanolamine. The Pi peak is now clearly separated from the PME and PDE peaks, facilitating the determination of localized pH. In addition to increased spectral resolution, the Nuclear Overhauser Effect (NOE) increases the sensitivity of the PME, PDE and PCr peaks in the ^{31}P spectra. Little or no increase is observed for ATP.

All data were acquired on a 1.5T Siemens Magnetom with normal volunteers, using a 3D CSI sequence with a 250 ms rectangular excitation pulse for ^{31}P and WALTZ 4 ^{1}H modulation. Observations times were 17 to 70 minutes depending upon the spatial resolution chosen which ranged from 64 (4x4x4) cm^3 to 27 (3x3x3) cm^3 and 18 (3x3x2) cm^3. Repetition time was 1 second and the ^{31}P pulse angle at the center of the coil was 40^0. Proton power levels were 15 watts during acquisition (0.256 seconds) dropping to a NOE maintenance level of 1.5 watts for the remaining 0.744 seconds. In addition to acquiring proton decoupled ^{31}P spectra, this coil can be used to acquire high quality proton images in the same examination, without repositioning the subject. The decoupled localized ^{31}P spectra produce improved metabolic images of the human brain. Overlaying the metabolic images on the proton images allows accurate anatomical referencing of the phosphorus spectra.

W-AM-D7

PENETRATION OF MONOCLONAL ANTIBODIES INTO TUMORS: A "BINDING SITE BARRIER"
John N. Weinstein, William W. van Osdol, and Kenji Fujimori, National Cancer Institute, NIH, Bethesda, MD 20892.

We have analyzed antibody penetration into a spherical cancer "micrometastasis" by splicing together information on (i) global pharmacokinetics, (ii) convective and diffusive transport across the blood capillary wall, (iii) diffusion through the tumor interstitial space, (iv) antigen-antibody interaction, (v) metabolism, and (vi) lymphatic outflow. The system of partial and ordinary differential equations describing these phenomena was solved numerically using a computer program that we call "PERC" (Weinstein, et al., Ann. N.Y. Acad. Sci. 507:199, 1987; Fujimori, et al., Ca. Res. 49:5656, 1989 and J. Nucl. Med. 31:1191, 1990). This analysis uses reasonable parameter values obtained from our own experimental studies and clinical trials at NIH, as well as from the literature. It predicts that 1) the very fact of successful antigen-antibody binding in tumors can retard antibody percolation to cells 50 or 100 μm from the blood vessel; 2) high antibody affinity at a given dose will tend to decrease antibody percolation because there are fewer free antibody molecules to diffuse. The result is a more heterogeneous distribution; 3) increasing antibody dose will lead to better percolation and more uniform distribution; 4) the radiation doses for radioimmunoconjugates will tend to be inhomogeneous microscopically if percolation is poor. Some of these predictions are borne out qualitatively by experimental findings and others remain to be tested.

We believe that the "binding site barrier" constitutes a major challenge to the molecular design of next-generation antibodies and also to the design of many other types of ligands for use in treatment of solid tumors. We also speculate that this barrier affects the evolutionary design of endogenous biological ligands such as the autocrine-paracrine factors. The authors gratefully acknowledge the Advanced Scientific Computing Laboratory, NCI/FCRF for supercomputer time and support.

W-AM-D8

NUMERICAL SOLUTION OF DIFFUSION EQUATIONS AS COUPLED FIRST ORDER LINEAR DIFFERENTIAL EQUATIONS
Izchak Z. Steinberg, Chemical Physics Department, Weizmann Institute of Science, Rehovot, Israel

Several problems involving linear diffusion processes were treated numerically by the following method. The space coordinate is subdivided into discrete elements, and the rate of change of the concentration with time at each of the spatial elements is expressed as a first order differential equation, the various equations being coupled to one another. This set of equations is solved by the diagonalization of the matrix of coefficients which appear in the above set of coupled equations and which have been derived from the original diffusion equation. This treatment yields a set of eigenvectors, each of which represents a specified spatial distribution of concentration in the range of interest. The amplitude of each of the eigenvectors decays monoexponentially with time, while retaining its shape, the lifetime of decay being the negative inverse of the corresponding eigenvalue. Any initial concentration distribution may be expressed as a linear combination of the set of eigenvectors, and the subsequent concentration distribution at any desired time later simply obtained by the algebraic summation of the surviving fractions of the above eigenvectors. This approach has some distinct advantages. One does not have to start the procedure from the beginning if new initial conditions are desired. The time dependence of the concentration distribution has an analytic form of multiexponential shape, the concentration distribution at any given instant thus being obtainable directly without the need of stepwise build-up of the solution with time. Thus, the asymptotic behavior of the changes in concentration at long times may be expressed as an exponential decay of the longest-lived eigenvector. Explicit reference will be made to intramolecular diffusion processes in polymer chains.

W-AM-D9

SIMULATION OF THE MOTION OF MICROVILLI-COATED HARD SPHERES ON SURFACES UNDER SHEAR FLOW: EFFECT OF SPHERE AND SUBSTRATE CHEMISTRY. Linda A. Tempelman and Daniel A. Hammer, School of Chemical Engineering, Cornell University, Ithaca, NY 14853.

When a cell such as a neutrophil, lymphocyte, or metastasizing tumor cell makes contact with the microvascular endothelium, cell surface asperities, such as microvilli, are thought to influence the adhesion of that cell by overcoming repulsive non-specific interactions between the cell and vascular wall. In addition, numerous observations of cell adhesion and rolling on surfaces indicate that transient adhesion, as evidenced by rapid fluctuations in the velocity of motion of cells, is quite common.

We have developed a simulation method to understand how microvilli might affect receptor-mediated cell adhesion under conditions of flow. In the simulation, we randomly distribute microvilli on the cell surface by modelling them as distributed patches on the surface of a sphere of a larger effective radius, and distributing receptors onto the microvillus tips using a Poisson distribution. Given typical estimates for the size of microvilli, and the numbers of receptor molecules on the surface, very small, integer numbers of receptors are likely to be found on any given microvillus, with wide variability between microvilli. Adhesion molecules on the microvillus tip are modeled as adhesive springs which sample all extensional and angular positions on a time scale shorter than the reaction time. The adhesion molecules react with the surface with reaction rates dependent on the mean distance of the microvillus tip to the surface. Random sampling in combination with probabilistic bond kinetics is used to assess the existence of bonds emanating from a particular microvillus. The orientation and number of bonds at each microvillus acts as a bonding contribution to the force and torque balances on the sphere, from which the translational and angular velocities of the sphere can be calculated. The simulations show how receptor-ligand affinity, receptor-ligand reaction rates, spring constant, numbers of receptors and microvilli, and flow rate all affect the rolling velocity, and determine how both the mean and standard deviation in the rolling velocity depend on these parameters.

We compare our analyses with several sets of data on cell and hard sphere adhesion in flow, including reports of transient contact, manifested by the variations in the instantaneous velocity from the mean, between cells and ligand-coated surfaces. Also, we compare our analysis to preliminary experimental results on the adhesion and rolling of rat basophilic leukemia cells sensitized with IgE molecules (bound to Fcε receptors on the cell surface) on antigen-coated surfaces.

W-AM-E1

MOLECULAR IMAGING OF THE CYTOPLASMIC SURFACE OF GAP JUNCTIONS

Tibbitts, T.T., D.A. Goodenough†, L. Makowski, J.S. Brooks. and S.T. Hannahs. Center for Molecular Biophysics, Dept. of Physics, Boston Univ., Boston, MA 02215 and †Dept. of Anatomy and Cell Biology, Harvard Medical School, Boston, MA 02115.

Elucidation of the molecular mechanisms of intercellular communication has depended upon structural characterization of the connexon hexamers which pair to form protein channel assemblies in gap junctions. The size and location of transmembrane α-helices in connexons has been determined by convolution modeling analysis of x-ray diffraction patterns from oriented membranes, but protein segments which protrude on the cytoplasmic face (approximately 100 of the 283 amino acids residues in the monomer) lack sufficent order to be characterized by this technique (Tibbitts *et.al.* 1990, *Biophys. J.* 57:1025-1036). Sensitivity of these domains to radiation has also limited their detailed analysis by transmission electron microscopy. Recently, we have obtained the first images of the cytoplasmic surface of gap junctions by scanning tunneling microscopy (STM). The membranes were deposited on highly oriented pyrolitic graphite and scanned in glycerol/water solutions without using metal coatings, Faradaic deposition of ions, or other special treatments. Two distinct types of ordered arrays have been imaged. The finer lattice, apparently a separated lipid phase, is resolved to better than 3.0 Å resolution. In some domains, alternating peaks of high and low conductivity are spaced 4.4 Å apart. The larger array has spacings more closely related to connexon lattice constants measured from x-ray diffraction patterns, but the features are less well resolved. Currently we are improving sample preparation and scanning techniques for high resolution difference imaging of native gap junction membranes and membranes treated with site-specific proteolytic enzymes.

W-AM-E2

THE TOPOLOGY OF MYELIN BASIC PROTEIN IN REVERSE MICELLES: A MEMBRANE MIMETIC SYSTEM.

Nicot, C., Vacher, M. and Waks, M. (Intro. by W. Urbach)
Département de Biochimie, UFR des Saints-Pères
Université Paris V - FRANCE

Proteolytic digestion can probe subtle changes in conformation of proteins and/or delineate the topology of membrane interacting proteins. Similar results can be obtained in the membrane-mimetic environment provided to membrane proteins by reverse micelles of AOT (sodium[2-bis ethylhexyl sulfosuccinate]), isooctane and water. To explore the interacting domains of myelin basic protein (MBP) - a major protein of the myelin sheath- with reverse micelle constituents, we have compared the results of limited proteolysis of MBP in buffer and in micellar solutions. The peptides were extracted, separated by high performance liquid chromatography (HPLC) and compared by gel electrophoresis and sequenced. Four different enzymes were assayed: trypsin, spleen cathepsin D, Staph. Aureus V8 protease and pepsin. In buffer, the digestion of MBP is total whereas in reverse micelles two large peptides Gly 107-Arg 129 and Ala 74-Arg 96 cleaved in buffer, were found inaccessible to trypsin. Furthermore, a monoclonal antibody with antigenic epitopes localized within the latter peptide sequence did not recognize MBP upon incorporation into reverse micelles, after the antigen-antibody binding was measured in buffer. For cathepsin D, Staph. Aureus V8 protease and pepsin, limited proteolysis reveal that the most accessible MBP peptide segments differ significantly in the aqueous and in the micellar media. We conclude that the folding of MBP in reverse micelles removes protein domains from proteolytic attack as a result of the multiple bonds formed between the micellar wall and the membrane protein. This protecting mechanism is disrupted in demyelinating processes such as multiple sclerosis.

W-AM-E3

THE TRANSIENT CHANGES IN CURVATURE OF PURPLE MEMBRANE FRAGMENTS AS A FUNCTION OF pH USING VISIBLE AND UV EXCITATION.

József Czégé and Lou Reinisch

Uniformed Services University of the Health Sciences, Bethesda, MD 20814

We have observed transient changes in the curvature of purple membrane fragments upon photoexcitation as a function of the pH of the suspending medium. The pH was varied from 4 to 11. The room temperature suspensions have low ionic strengths, and the bending is observed by changes in the scattered light at 320 nm. The changes in the scattered light are monitored from 2.5 μs to 1 s. When the photocycle is initiated with a visible laser pulse at 532 nm, three fundamental bending processes are observed in the scattering transients. However, when the sample is excited with a U.V. laser pulse at 355 nm at most two transient bending processes are observed. We use a simple first order approximation to subtract away any changes in the scattered light associated with transient absorption changes during the photocycle. The resultant curves are fit to the sum of three fundamental bending processes. Each process has an exponential rise, an exponential decay and an amplitude. Possible origins of the bending processes are discussed.
This work has been supported, in part, by a grant from the Office of Naval Research, grant N00014-WR-24020.

W-AM-E4

PURIFICATION AND CHARACTERIZATION OF A CANDIDATE AMINOPHOSPHOLIPID FLIPPASE.

David L. Daleke, Kathleen A. Cornely-Moss, and Christine M. Smith. Department of Chemistry, Indiana University, Bloomington, IN 47405.

Biological membranes possess a non-random distribution of phospholipids across the bilayer; PE and PS are primarily located on the cytoplasmic surface, while PC and SM are found predominantly on the membrane outer surface. Transmembrane phospholipid asymmetry is maintained in part by vanadate-sensitive, Mg^{2+}-ATP-dependent transport of PS and PE from the outer to inner membrane surface. We have partially purified a Mg^{2+}-ATPase from human erythrocytes that has properties similar to the aminophospholipid transporter. Using a combination of ammonium sulfate precipitation, Mono Q FPLC, hydroxylapatite chromatography, gel exclusion chromatography, and density gradient centrifugation, we have obtained a partially purified preparation containing seven major proteins (137, 120, 84, 48, 40, 35 and 31 kDa). The detergent solubilized protein mixture exhibits vanadate-sensitive, PS-dependent ATPase activity. The 120 kDa protein is selectively labeled by ATP-γ-^{35}S and may be the ATPase. ATPase activity is inhibited by sulfhydryl reagents and phenylglyoxal, effective inhibitors of aminophospholipid transport in intact cells. The partially purified protein is activated by PS and PE, but not by PC, PG, PA, or fatty acids. Several PSs stimulate ATPase activity and a slight dependence of activity on PS acyl chain composition is observed (POPS > brain PS > DOPS > DLPS > NBD-PS). PS-stimulated ATPase activity is greater in the presence of cholesterol, indicating that cholesterol may have a modulating effect on enzyme activity. ATPase activity is activated by PI and lyso PS, lipids that are not substrates for the transporter in intact cells, implying that the ATPase activity of the transporter may have unique lipid requirements or that another ATPase is present in our preparation.

W-AM-E5

WHAT DETERMINES THE SIZE OF PHOSPHOLIPID VESISCELS MADE BY DETERGENT-REMOVAL TECHNIQUES?

M. Rotenberg and D. Lichtenberg, Department of Physiology and Pharmacology, Sackler Faculty of Medicine, Tel Aviv University, Ramat Aviv, 69978 ISRAEL

Vesicles made by infinite dilution of mixed micelles of PC and the non-ionic detergent octylglucoside (OG) have a mean diamter of about 50nm. The use of other detergents, non-ionic (Triton X-100), Zwitteronic (CHAPS), anionic (cholate) or cationic (CTAB), results in much smaller vesicles with diameters within the range of 22-30nm. The small variation in the size of the latter vesicles indicates that the micelles vesicles transformation occurs through closure of discordial, cylindrical or elipsoidal mixed micelles when these structures are sufficiently large to reduce the energy of curving to the absolute value of the "edge energy" associated with exposure of "hydrophobic core" to water.

When formation of vesicles is brought about by slower detergent-removal techniques, post-vesiculation, detergent-induced, size growth is probably responsible for the formation of larger vesicles. Thus, the ultimate size of vesicles made by detergent removal depends on the rate of the post-vesiculation size growth processes relative to the rate of detergent removal. The apparently unique characteristics of OG as compared to other detergents may results from an extremely rapid vesicle size growth, which may, in turn, be a consequence of the macroscopic phase separation of PC-OG mixed micelles from vesicles within the range of co-existance of these two types of aggregates.

W-AM-E6

SCANNING ELECTRON MICROSCOPY OF HYDRATED OR DRIED LANGUMIR LIPID FILMS

Klaus-Ruediger Peters, Roderike Pohl and David G. Rhodes, Biomolecular Structure Analysis Center, Department of Radiology, University of Connecticut Health Center, Farmington, CT

Two nev electron microscopic imaging technologies were used to assess molecular structure and physical properties of Langumir lipid films. The environmental scanning electron microscope (ESEM: ElectroScan ESEM-E3) was used to examine fully hydrated films supported by the aquous subphase and the ultrahigh resolution field emission scanning electron microscope (FSEM: JEOL JSM-890) was used to image stabilized and dried films. Langumir films were made from DPPC or from pulmunary surfactant lipid extracts. The films were compressed to a solid-like phase (π=30 dyne/cm) in a Teflon trough with a Delrin barrier (KSV 5000), and were supported by 2000 mesh platinum grids. The fully hydrated monomolecular lipid films were imaged in the ESEM with the secondary electron signal at saturated water vapor pressures without processing or metal coating. The fine regulation of temperature and water vapor pressure allowed controlled water condensation on the film surfaces. The extent of condensation pattern continuity allowed easy determination of lipid orientation in the monolayers. For dried films, film integrity during drying could be maintained through chemical stabilization, dehydration by freeze-substitution and freeze drying. Dried films were investigated without metal coating in the ESEM or after coating in the FSEM. The FSEM allowed high magnification imaging at a molecular (~nm) level. The technologies will be used for investigation of lipid micro domains and protein/lipid interactions.

We thankfully acknowledge the gift of surfactant lipid extracts by Dr. Robert H. Notter, University of Rochester, Rochester, NY, and the imaging support obtained from ElectroScan, Wilmington, MA. Supported by Connecticut Department of Higher Education Grants 89-317, H3-89, H38-90 and NSF Grants DIR-8907117, CTS-8904938.

W-AM-E7

STRUCTURAL INVESTIGATION OF LIPID MONOLAYERS AND LIPID/PROTEIN SURFACE LAYERS UTILIZING THE NEUTRON REFLECTION TECHNIQUE

D. Vaknin*, J. Als-Nielsen*, K. Kjær*, and M. Lösche#

*Physics Dept., Risø Natl. Lab., DK-4000 Roskilde, Denmark
#Inst. Phys. Chem., Univ. Mainz, D-6500 Mainz, Germany

The structure of DPPC monolayers on top of ultrapure H_2O and D_2O subphases has been investigated by measuring the angular dependence of the neutron reflectivity directly on a Langmuir film balance. Using a dedicated liquid surface reflectometer,[1] we have been able to access reflectivities down to R = 10^{-6} in the momentum transfer range Q_z = 0 - 0.4 Å^{-1}.

The isotherms show a pronounced isotope (H_2O/D_2O) effect that is attributed to an increased strength of deuteron bonds to the lipid head groups as compared to hydrogen bonds.

For the highly condensed phase of chain-perdeuterated DPPC-d_{62} we have compared our results from both, H_2O and D_2O, subphases with X-ray results[2] and found a unique model that fits all three data sets. We find the head group layer interpenetrated with subphase water (approx. 4 to 6 molecules of D_2O per lipid head group). This model includes the presence of an additional layer of water of reduced (by ~ 10%) density beneath the head group layer. In the fluid state we observe (a) a reduction of tail region thickness and scattering length density which is consistent with the common model of a transition to a less ordered phase and (b) an increase of head group water content.

At present, binding studies of streptavidin to biotin substituted lipid species anchored in a DPPC surface film are under way.

[1]D. Vaknin, K. Kjær, and J. Als-Nielsen, manuscript in preparation

[2]C.A. Helm, H. Möhwald, K. Kjær, and J. Als-Nielsen, Europhys. Lett. 4 (1987), 697-703.

W-AM-E8

DEUTERIUM NMR STUDIES OF CURVATURE, ORDER, AND DYNAMICS OF PHOSPHATIDYLETHANOLAMINE DISPERSIONS. Robin L. Thurmond, Göran Lindblom, and Michael F. Brown. *Department of Chemistry, University of Arizona, Tucson, AZ 85721.*

The presence of **inverse hexagonal phase**, H_{II}, favoring lipids in membranes has been suggested to be important in many biological processes.[1] Therefore an understanding of the H_{II} phase and the bilayer to hexagonal transition is of importance. Deuterium (^{2}H) NMR spectroscopy allows for study of the orientational order and dynamics of lipids at the molecular level, and can add significant insight into the structure and behavior of the H_{II} phase. We have used ^{2}H NMR spectroscopy to investigate the bilayer and inverse hexagonal phases of 1-perdeuteriopalmitoyl-2-linoleoyl- *sn* -glycero- 3 -phosphoethanolamine. The difference in organization between the two phases is accompanied by smaller segmental **order parameters**, S_{CD}, and higher transverse, R_2, **relaxation rates** for the H_{II} phase compared to the L_α phase. Because these quantities are sensitive to the geometry of the aggregates they can be used to extract structural information about the phases. We have calculated average acyl chain lengths and chain cross-sectional areas for both phases, and indicate how the difference in these values can be related to the curvature for the H_{II} phase. These measurements are in agreement with and extend current understanding of the structure of the H_{II} phase. [1]T.S. Wiedman *et al.* (1988) *Biochemistry* **27**, 6469. Lindblom *et al.* (1986) *Biochemistry* **25**, 7502. Work supported by the NIH (GM41413, EY03754, and RR03529).

W-AM-E9

EFFECTS OF ANESTHETICS ON MODEL MEMBRANE SYSTEMS: INFLUENCE OF ONE-SIDED ATTACK. Robert E. Cunningham, Maureen Ngoh, Amy Williamson, Walter Engler and Timothy J. O'Leary, Department of Cellular Pathology, Armed Forces Institute of Pathology, Washington, DC 20306-6000.

We investigated the effects of normal alcohols ranging in size from one carbon atom (methanol) to fourteen carbon atoms (cis- *and trans*-tetradecenols) on the leakage of dioleoylphosphatidylcholine (DOPC) vesicles using the quenching of 8-aminonaphthalene-1,3,6-trisulfonic acid (ANTS) by p-xylene-bis-pyridinium bromide (DPX) as a probe. When vesicles leak, DPX no longer quenches ANTS fluorescence, and overall solution fluorescence increases. Short chain alcohols were dispersed directly into a 2.5 ml solution of MOPS buffer. Longer chain alcohols (hexanol and above) were dispersed into ethanol; the final ethanol concentration was substantially below that which causes vesicle leakage. Vesicles were injected into the MOPS/alcohol solution; this resulted in an immediate increase in the solution fluorescence, due to the addition of incompletely quenched ANTS. When leakage occurred, a further increase in fluorescence, not observed in control solutions, was observed over the next few minutes. For all alcohols, the leakage and anesthetic concentrations were within a factor of 10 of each other. For the *cis-* and *trans-* tetradecenols, lower concentrations were needed for leakage than for anesthesia, but ethanol concentrations may have been high enough (up to 0.3M) to influence the results. Electron microscopic images of the alcohol-vesicle solutions demonstrated that significant morphologic changes occurred in the vesicles at the alcohol concentrations causing vesicle leakage. These seem to correspond to fusion, then breakup. Nevertheless, intact vesicles can be formed when the vesicles are initially hydrated in water-alcohol solutions at concentrations which cause vesicle lysis in the above experiment, where the alcohol is added to only one side of the vesicle membrane. This experiment suggests that greater structural perturbations may be produced by anesthetics when they approach the lipid membrane from only one side, rather than from both.

W-AM-F1

DIRECT MEASUREMENT OF LIGAND-RECEPTOR INTERACTIONS

C. A. Helm*†, W. Knoll* and J. N. Israelachvili*

†Institut für physikalische Chemie, Johannes Gutenberg Universität, Jacob-Welder Weg 11, D-6500 Mainz, Germany
*Department of Chemical & Nuclear Engineering, and Materials Department, University of California, Santa Barbara, CA 93106, USA
*Max-Planck Institut für Polymerforschung, Postfach 3148, D-6500 Mainz, Germany

During the past 20 years the fundamental forces between surfaces in liquids have been systematically studied both experimentally and theoretically. The main forces, e.g. van der Waals, electrostatic, hydrophobic, are not system-specific in the sense that the interaction potential is rather determined by the physical properties (charge, dielectric constant, etc) than by the specific chemical composition of the system. Hence the force is a known function of distance, such as a power law or exponential function. Less studied is a specific binding mechanism between certain molecules. Such ligand-receptor interactions give rise to very strong bonds due to perfect geometrical fit. Using the Surface Forces Apparatus we have studied the interactions between membrane-bound Biotin ligands and Streptavidin receptors. We find an unusually strong short-range binding force associated with equally specific molecular rearrangements - both qualitatively and quantitatively unlike anything previously measured. Nature has here developed an extremely efficient mechanism whereby noncovalent adhesive junctions can be switched on, or mechanically "locked", quickly and with minimal expenditure of energy.

W-AM-F2

BRIGHT FLUORESCENT PROBE FOR HIGH PRECISION TRACKING OF INDIVIDUAL IMMUNOGLOBULIN E RECEPTOR MOLECULES

James P. Slattery, David Holowka, Richik Ghosh, Watt W. Webb, and Barbara Baird, Cornell Univ., Ithaca, NY

We are developing a general method for microscopic tracking of individual receptor molecules on the surface of living cells using monoclonal antibodies or their monovalent Fab fragments conjugated to fluorescently labeled low density lipoprotein (LDL). In our initial effort we have chosen a monoclonal anti-immunoglobulin E (IgE) antibody (B5) that binds to the $F(ab')_2$ region of IgE with a 1:1 stoichiometry. After modification with succinimidyl 3-(2-pyridylthio)propionate (SPDP) this antibody is reacted with LDL that has been previously labeled with the fluorescent carbocyanine probe, 1,1'-dioctadecyl-3,3,3',3'-tetramethylindocarbocyanine perchlorate ($DiIC_{18}$), then modified with SPDP and reduced with dithiothreitol. The covalent 1:1 conjugates of B5-$DiIC_{18}$-LDL are recovered by floatation in the ultracentrifuge and appear to label IgE-receptor complexes on the surface of rat basophilic leukemia cells in a specific, non-perturbing manner. Quantitative low-light level digital video microscopy has been used for high precision tracking of individual labeled receptors. Plots of mean-squared displacement *vs* time for preliminary tracking data indicate three modes of motion: diffusion, diffusion superimposed on a drift velocity, and percolation. Individual receptors can switch between two modes of motion during a single experiment. Supported by grants from NIH (AI18306 and AI22449 to DH and BB and 5P41RR04224 to WWW) and NSF (DIR8800278 to WWW).

W-AM-F3

THE 50 kD SUBUNIT OF THE DYSTROPHIN-GLYCOPROTEIN COMPLEX IS LOCALIZED TO BOTH THE SURFACE SARCOLEMMA (SL) AND TRANSVERSE (T)-TUBULES IN RABBIT VENTRICULAR MYOCYTES. R. Kletsch*, W. Arnold*, A.C.-Y. Shen*, K.P. Campbell‡ and A.O. Jorgensen*, *Dept. of Anatomy, Univ. of Toronto, Toronto, Canada; ‡Dept. of Physiol. & Biophysics, University of Iowa, Iowa City, IA.

It has previously been reported that dystrophin is localized at the surface SL of both skeletal and cardiac muscle. To determine whether the 50 kD glycoprotein subunit (SL50) of the dystrophin-glycoprotein complex and TS28 respectively markers of surface (SL) and (T) tubules of skeletal muscle (Jorgensen et al J.Cell Biol. 110:1173 (1990) and Ervasti et al Nature 345:315 (1990)) are also specific markers of surface SL and T-tubules in cardiac muscle the subcellular distribution of these two proteins in rabbit ventricular myofibers were studied by immunofluorescence and immunocolloidal gold labeling of tissue sections. The results showed that mAb IVD3, to SL50 and mAb $IXE11_2$ to TS28 respectively recognized a 50 kD (H50) and a 68 kD (H68) protein in a cardiac muscle extract. As anticipated, H50 and H68 were confined to distinct but continuous domains of the cardiac muscle cell surface. However, the two domains were not those corresponding to surface SL and T-tubules in cardiac muscle. Instead H50 was observed to be present in regions of the cell surface corresponding to both surface SL and T-tubules. As expected, H68 was absent from the surface SL however, it was also absent from T-tubules. Instead, H68 was present in discrete clusters in the subsarcolemmal region of the intercalated disc, possibly corresponding to caveolar-like structures in this region of the SL. Thus with respect to protein composition, it appears that skeletal surface SL has characteristics in common with both surface SL and T-tubules in cardiac muscle not shared by skeletal T-tubules. Furthermore, the skeletal T-tubular function specified by TS28 appears to be absent from the cardiac T-tubules and instead reside in H68 localized to subsarcolemmal invaginations of the surface SL.

W-AM-F4

OLFACTORY RECEPTORS SHARE ANTAGONIST HOMOLOGY WITH OTHER G-PROTEIN COUPLED RECEPTORS. Stuart J. Firestein and Gordon M. Shepherd, Section of Neuroanatomy, Yale Medical School, New Haven, CT.

In olfactory receptor neurons, non-hydrolyzable analogs of GTP and GDP, respectively, prolong and attenuate the ionic current elicited by odor stimuli, supporting a G-protein-receptor coupled mechanism in olfactory transduction. However, the odor receptor protein coupled to the G-protein has thus far eluded detection. Other signal transduction systems utilizing G-proteins share many common features; for example the G-protein is often coupled to a membrane protein receptor with seven transmembrane spanning regions. Among these, rhodopsin, muscarinic and β-adrenergic receptors show significant homology and are generally presumed to be members of a superfamily of receptor proteins. We hypothesized that the putative olfactory receptor might share sufficient homology with other members of this family that some antagonists might also effect olfactory receptors. The muscarinic antagonists atropine, scopolamine and QNB, applied extracellularly in concentrations of 20-200 uM, acted as reversible, partial antagonists, attenuating the odor elicited current by one-third to one-half. The inhibitory EC50 ranged from 70-100 uM. Muscarine, at similar concentrations, had no direct effect on the cell but also antagonized the odor response. The β-adrenergic receptor antagonist propranolol was more effective, blocking the odor response at a concentration of 80 uM with an EC50 of 20 uM. The concentrations used for both types of antagonists were considerably higher than those effective in the native systems but no non-specific effects, such as alterations in input resistance, resting potential or voltage gated currents, were observed. These preliminary data suggest that olfactory transduction involves a protein receptor which may be a member of the family of seven membrane spanning, G-protein coupled receptors. Additionally these pharmacological agents may prove experimentally valuable, since there are currently no known olfactory antagonists.

Supported by Office of Naval Research, NINDS and NIDCD.

W-AM-F5

ADRENERGIC AGONISTS RELEASE INTRACELLULAR CALCIUM IN HELA CELLS TRANSFECTED WITH α_1-ADRENERGIC RECEPTOR CLONES. J. M. Rendt and D. A. Schwinn, Curriculum in Neurobiology, Univ. of North Carolina, Chapel Hill, NC; Dept of Anesthesiology, Duke University Medical Center, Durham, NC.

We have characterized the electrical response of HeLa cells expressing different subclones of the α_1-adrenergic receptor. In cells expressing the α_{1B} (Cotecchia, *et al.*, PNAS 85:7159, 1988) or the α_{1C} (Schwinn, *et al.*, J. Biol. Chem 265:8183, 1990) subclones, 10^{-4} M norepinephrine (NE) increases **total** inositol phosphate (IP) isomers by 196±34% (n=11) and 696±97% (n=11), respectively; the EC_{50} is 7.44 μM and 21.88 μM for the α_{1B} and the α_{1C} respectively. (Schwinn, *et al.*, In preparation).

To determine if the increase in IP was sufficient to release calcium from internal stores, we have measured the activity of calcium-activated potassium channels (K_{Ca}) using the whole-cell patch-clamp method. Application of 50 μM NE or 50 μM phenylephrine (PE) causes an outward K current as determined by its reversal potential. With continued application the current decreases with a half-time of 1 min. The response could be reinitiated after 3-5 mins in agonist-free solution. The response was not abolished when agonist was applied in a calcium-free solution. Application of 1 mM caffeine caused a qualitatively similar increase in outward current.

Spontaneous outward currents were sometimes seen in agonist free solution after an initial application of agonist. Occasionally, oscillations in the outward current were seen during agonist application.

Supported by NS-18788

W-AM-F6

Adenosine Deaminase in Cell Transformartion: Biophysical Manifestation of membrane dynamics.

Abraham H. Parola

Department of Chemistry, Ben-Gurion University of the Negev
P.O. Box 653, Beer-Sheva, Israel.

The role of membrane lipid-protein interactions in malignant cell transformation was examined with adenosine deaminase (ADA) as a representative membrane protein. ADA's activity changes dramatically in transformed cells and accordingly it is a malignancy marker. Yet, the mechanisms controlling its variable activity are unkown. We undertook the spectroscopic deciphering of its interactions with its lipidic environment in normal and malignant cells.

ADA exists in two interconvertible forms, small (45 KD) and large (210 KD). The large form consits of two small catalytic subunits (SS-ADA) and a dimeric complexing protein ADCP. The physiological role of ADCP was not known either.

Our studies were carried out at three levels: 1. Solution enzyme kinetics, 2. The interaction of SS-ADA with ADCP reconstituted in liposomes: Effect of cholesterol and 3. Multifrequency phase modulation spectrofluorometry of pyrene-labeled SS-ADA bound to ADCP on the membranes of normal and RSV or RSV Ts68 transformed chick embryo fibroblasts.

We found: 1. ADCP has an allosteric regulatory role on SS-ADA, which may be of physiological relevance: it inhibits SS-ADA activity at low physioligical adenosine concentrations but accelerates deamination at high substrate concentration.

2. When reconstituted in DMPC liposomes, it retains SS-ADA activity (in its absence the activity is lost) and upon rigidification with cholesterol, a threefold increase in SS-ADA activity is attained, contrary to ADCP's regulatory activity when free of lipids.

3. The reduced ADA activity in transformed chick embryo fibroblasts is associated with increased membrane lipid fluidity (reduced order parameter), reduced accesibility of ADCP and increased rotational dynamics of the complex. We thus obtained spectroscopic deciphering of the vertical motion of ADCP, controlled by lipid-protein interaction, resulting in variable activity of this malignancy marker.

W-AM-F7

THE CELL SURFACE RECEPTOR TRANSPORT IN A.C. ELECTRIC FIELDS IS CELL SHAPE DEPENDENT. Gowrishankar, T.R.; Patel, P.K., Lee, R.C. and *Golan, D.E., Depts. of Surgery and Organismal Biology, Univ. of Chicago, Chicago, Il. 60637 and *Dept. of Biological Chem. & Pharmacology, Harvard Medical School, Boston 02115

Clustering or aggregation of cell surface receptors is an important intermediate step in the cellular processing of certain types of ligands. Under applied electric fields receptor transport is governed by dynamic balance between mutual diffusion and migration by electrophoresis and electroosmosis. If the resistance to receptor transport is uniaxially anisotropic, then receptor migration under sinusoidal electric fields would result in net time-average receptor displacement, effectively rectifying the receptor displacement. Because the spatial and temporal modes of mutual diffusion are dependent on surface geometry, we postulated that certain non-spherical cell shapes lead to uniaxial anisotropic resistance to receptor transport. To test this hypothesis we used the finite difference method to numerically solve the convection-diffusion equation describing transport of cell surface receptors. We modeled the balance between electrophoresis and diffusion of charged surface receptors using measured values for class II MHC receptor diffusivity(1.5×10^{-9} cm^2/s) and mobility(7.5×10^{-7} cm^2/V-s) on the surface of human fibroblasts in monolayer culture. A 2-D mesh was derived from photomicrographs of the cells. Bidirectional transport along the cell's major axis in a 1-10V/cm sinusoidal electric fields aligned parallel to the axis was simulated. The simulation was performed over a frequency range spanning two orders of magnitude above and below the reciprocal average mutual diffusion relaxation time. Effects of receptor crowding and excluded volume were included by using published finite radius values for the receptors.

Sinusoidal electric fields produced a time-average accumulation of receptors at the tapered ends of cell processes which was as large as 70% greater than the initial concentration. This rectification was dependent on the rate of geometrical taper. Uniaxial anisotrophy of receptor movement is a natural consequence of a non-symmetrical cell shape and is consistent with anisotropic back-diffusion that we have previously demonstrated [1]. This mechanism of rectification may underlie the reported sensitivity of non-spherical cells to sinusoidal electric fields.

[1] Basch, RM, M.S.Thesis, M.I.T., 1987 (R.Lee & D.Golan, supervisors).

W-AM-F8

MODULATION OF ETHIDIUM BINDING TO THE NICOTINIC ACETYLCHOLINE RECEPTOR BY GENERAL ANESTHETICS AND COBRA-α-TOXIN

C. Fernando Valenzuela, James A. Kerr, David A. Johnson, Division of Biomedical Sciences, Univ. of Calif., Riverside CA 92521-0121.

The muscle-type nicotinic acetylcholine receptor (AcChR) is a ligand-gated ion channel. Ligands interact with the AcChR at three classes of binding sites: the agonist/competitive antagonist, the high-affinity noncompetitive inhibitor (NCI), and the low-affinity NCI binding sites. Agonists and high-affinity NCIs preferentially bind to and stabilize the AcChR in a desensitized state. Low-affinity NCIs such as general anesthetics (GA) can enhance the binding of ligands to the high-affinity NCI binding site. Competitive antagonists, like cobra α-toxin, do not block alcohol induced histrionicotoxin binding to the high-affinity NCI binding site. To further evaluate the interrelations between ligand binding sites, we examined the effect of GAs and cobra-α-toxin on ethidium binding to the high-affinity NCI binding site by using spectrofluorometeric techniques. Ethidium was selected, because it preferentially binds to the desensitized receptor and displays large changes in emission upon binding. Halothane, ether, and butanol induced and alphaxalone and thiamylal had no effect on phencyclidine-sensitive ethidium binding. The presence of α-toxin blocked the anesthetic-induced increase in ethidium binding. We found that 1) some but not all GAs increase ethidium binding to the high affinity NCI binding site and 2) the GA-induced binding of high-affinity NCIs can be blocked by α-toxin. These results support the idea that snake α-toxins act both as competitive inhibitors of agonist binding as stabilizers of the AcChR-resting state.

(Supported by NSF grant BNS-8821357)

W-AM-F9

ANTIBODY INDUCED CHANGES IN THE "A" AND "B" BINDING SITES FOR ACETYLCHOLINE ON THE TORPEDO RECEPTOR.

David A. Johnson, Phi Weign, and Alan J. Dowding. (Intro. by Paul M. Quinton) Univ. of Calif., Riverside, CA 92521-0121 and MRC Cell Biophysics Unit, London WC2B 5RL, U.K.

We examined the effects of some of the monoclonal antibodies, developed by Dowding and Hall [*Biochemistry*, 26, 6372-81] that selectively inhibit ligand binding to either the "A" or the "B" acetylcholine binding sites, on the pharmacological and spectral properties of Dansyl-C_6-Choline bound to the unblocked acetylcholine binding site. We observed that the site-specific monoclonal antibodies produced the following effects: (1) a 1.4 to 2.1-fold increase in the magnitude of fluorescence resonance energy transfer between receptor tryptophans and the receptor-bound Dansyl-C_6-choline, (2) a 3.5 to 5-fold reduction of the binding affinity of the Dansyl-C_6-choline toward either the "A" or the "B" acetylcholine binding sites, (3) a 2 to 2.5-fold increase in the quantum yield of Dansyl-C_6-choline bound to the "A" or "B" binding sites, (4) a 10 nm blue shift in the emission spectrum of Dansyl-C_6-choline only when the "A" type monoclonal antibody interacted with the receptor, and (5) a change in the concentration, not the ability, of carbamylcholine to induce ethidium to bind to the high-affinity noncompetitive inhibitor site on the receptor. Coupled with our previous observation that the interaction of these antibodies with the receptor is associated with a greater distance of closest approach between the acetylcholine binding sites and the surface of the lipid membrane, these results show that the monoclonal antibodies change the agonist-induced conformation of the receptor. In the presence of agonists, the antibody-associated receptor conformation may be similar to the single site-occupied receptor or to a nonphysiological conformation.
(Supported by NSF grant BNS-8821357)